Chapter 7

Descriptive Crystal Chemistry

Crystal chemistry is concerned with the structures of crystals. It is to be distinguished from crystallography which is mainly concerned with the experimental methods used to solve crystal structures. Crystal chemistry includes topics such as: the description and classification of crystal structures, the factors that govern which type of structure is observed for a particular composition, and vice versa, the conditions under which a particular type of crystal structure is observed and the relation between crystal structure and physical or chemical properties.

This chapter and the next aim to cover the pertinent points of crystal chemistry. It is not intended to give a comprehensive survey of crystal structures as excellent reference works are available for this (e.g. Wells, 1984; Wyckoff, 1971; *Structure Reports*) and, anyway, space is strictly limited. Instead, a few of the more important structure types are discussed in some detail in this chapter and emphasis is given to the different ways in which a particular structure may be

described and classified. In the next chapter, the factors which influence crystal structures are considered.

7.1 Description of crystal structures

Crystal structures may be described in various ways. The most common way, and one which gives all the necessary information, is to refer the structure to the unit cell (Section 5.3.1). In this approach, the structure is given by the size and shape of the cell and the positions of the atoms inside the cell. However, a knowledge of the unit cell and atomic coordinates alone is often insufficient to give a revealing picture of the structure in three dimensions. This latter is obtained only by considering a larger part of the structure, comprising perhaps several unit cells, and by considering the arrangement of atoms relative to each other, their coordination numbers, interatomic distances, types of bonding, etc. From this more general view of structures, it is possible to find alternative ways of visualizing them and also to compare and contrast different types of structure.

Two of the most useful ways of describing structures are the *close packing* approach and the *space filling polyhedron* approach. Neither of these can be applied to all types of structure and both have their advantages and limitations. They do, however, provide a much greater insight into crystal chemistry than is obtained using unit cells alone.

7.1.1 Close packed structures—cubic close packing (c.c.p.) and hexagonal close packing (h.c.p.)

Many metallic, ionic, covalent and molecular crystal structures can be described using the concept of close packing. The guiding factor is that structures are arranged so as to have the maximum density, although this needs some qualification when ionic structures are being discussed. The principles involved can be understood by considering the most efficient way of packing together in three dimensions, equal-sized spheres.

The most efficient way of packing spheres in *two* dimensions is as shown in Fig. 7.1. Each sphere, e.g. A, is surrounded by, and is in contact with, six others. By regular repetition, infinite sheets called *close packed layers* are formed. The coordination number of six is the maximum possible for a planar arrangement of contacting, equal-sized spheres. Lower coordination numbers are, of course, possible, as shown in the inset in Fig. 7.1, but in such cases the layers are no longer close packed. Note also that within a close packed layer, three *close packed directions* occur. In Fig. 7.1, rows of spheres in contact occur in the directions XX′, YY′ and ZZ′ and sphere A belongs to each of these rows.

The most efficient way of packing spheres in *three* dimensions is to stack close packed layers on top of each other to give *close packed structures*. There are two simple ways in which this may be done, resulting in *hexagonal close packed* and *cubic close packed* structures. These are derived as follows.

The most efficient way for two close packed layers A and B to be in contact is

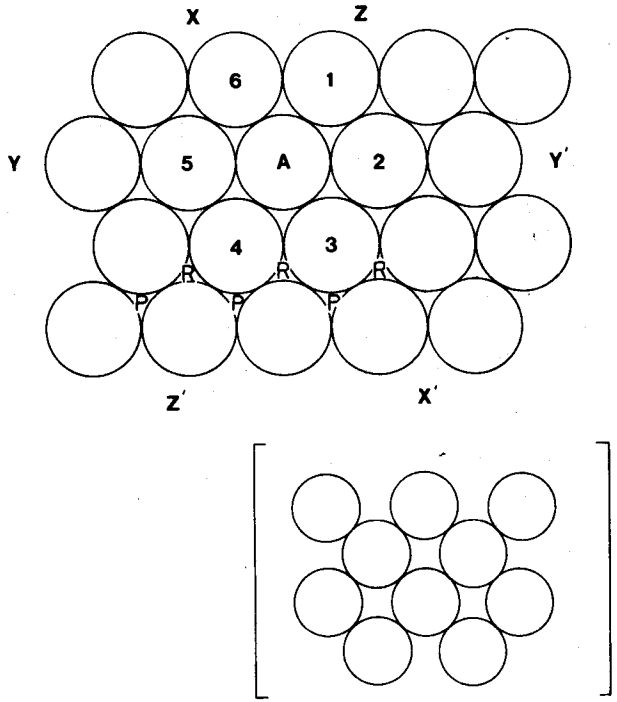

Fig. 7.1 A close packed layer of equal-sized spheres. Inset shows a non-close packed layer

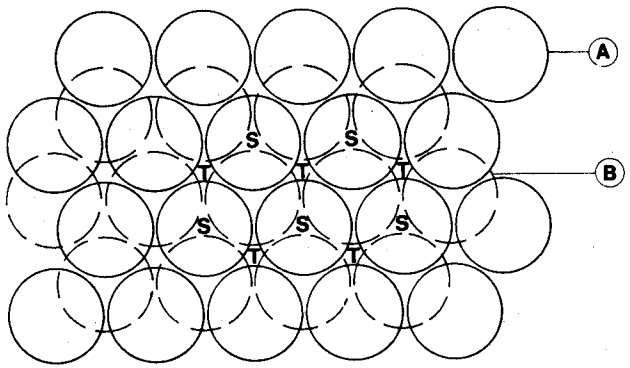

Fig. 7.2 Two close packed layers arranged in A and B positions. The B layer occupies the P positions shown in Fig. 7.1

for each sphere of one layer to rest in a hollow between three spheres in the other layer, e.g. at P or R in Fig. 7.1. Two layers in such a position relative to each other are shown in Fig. 7.2. Atoms in the second layer may occupy either P or R positions, but not both together, nor a mixture of the two. Any B (dashed) sphere is therefore seated between three A (solid) spheres, and vice versa.

Addition of a third close packed layer to the two shown in Fig. 7.2 can be done in two possible ways and herein lies the distinction between hexagonal and cubic close packing. In Fig. 7.2, suppose that the A layer lies underneath the B layer and we wish to place a third layer on top of B. There is a choice of positions for this third layer as there was for the second layer: the spheres can occupy either of the new sets of positions S or T but not both together nor a mixture of the two. If the third layer is placed at S, then it is directly over the A layer. As subsequent layers are added, the following sequence arises:

...ABABAB...

This is known as *hexagonal close packing*. If, however, the third layer is placed at T, then all three layers are staggered relative to each other and it is not until the fourth layer is positioned (at A) that the sequence is repeated. If the position of the third layer is called C, this gives (Fig. 7.3):

...ABCABCABC...

This sequence is known as *cubic close packing*.

Hexagonal close packing (h.c.p.) and cubic close packing (c.c.p.) are the two simplest stacking sequences and are by far the most important in structural chemistry. Other more complex sequences with larger repeat units, e.g. ABCACB or ABAC, do occur in a few materials; some of these larger repeat units are related to the phenomenon of polytypism (see later).

In a close packed structure each sphere is in contact with *twelve* others and this is the maximum coordination number possible for contacting and equal-sized spheres. (A common non-close packed structure is the body centred cube, e.g. in α-Fe, with a coordination number of eight; see Fig. 5.24a.) Six of these neighbours

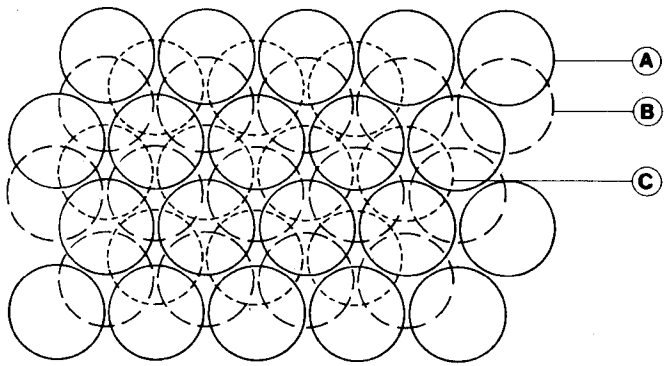

Fig. 7.3 Three close packed layers in c.c.p. sequence

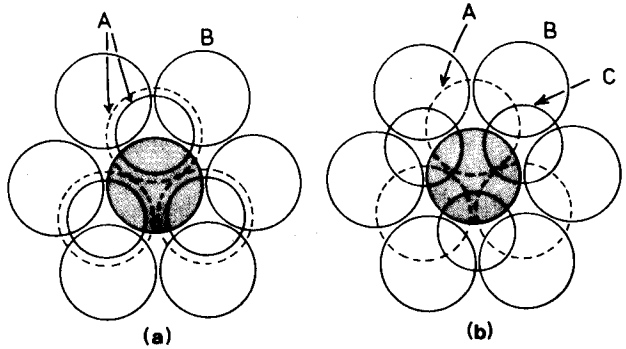

Fig. 7.4 Coordination number 12 of shaded sphere in (a) h.c.p. and (b) c.c.p. structures

are coplanar with the central sphere (Fig. 7.1) and from Figs 7.2 and 7.3 the remaining six are in two groups of three spheres, one in the plane above and one in the plane below (Fig. 7.4); h.c.p. and c.c.p. differ only in the relative orientations of these two groups of three neighbours.

The unit cells of cubic close packed and hexagonal close packed structures are given in Figs 7.5 and 7.6. The unit cell of a c.c.p. arrangement is the familiar face centred cubic (f.c.c.) unit cell (Fig. 7.5a) with spheres at corner and face centre positions. The relation between c.c.p. and f.c.c. is not immediately obvious since the faces of the f.c.c. unit cell do not correspond to close packed (c.p.) layers: thus, each face centre sphere has only four equidistant neighbours at the corners of the unit cell, as in the inset in Fig. 7.1. The c.p. layers are, instead, parallel to the {111} planes (Section 5.3.6) of the f.c.c. unit cell. This is shown in Fig. 7.5(b) by removing sphere 1 from its corner position to reveal part of a close packed layer underneath (compare (b) with Fig. 7.1): the orientations of (a) and (b) are the same but the spheres in (b) are shown larger and almost contacting. A similar arrangement to that shown in (b) would be seen on removing any corner sphere and, therefore, in

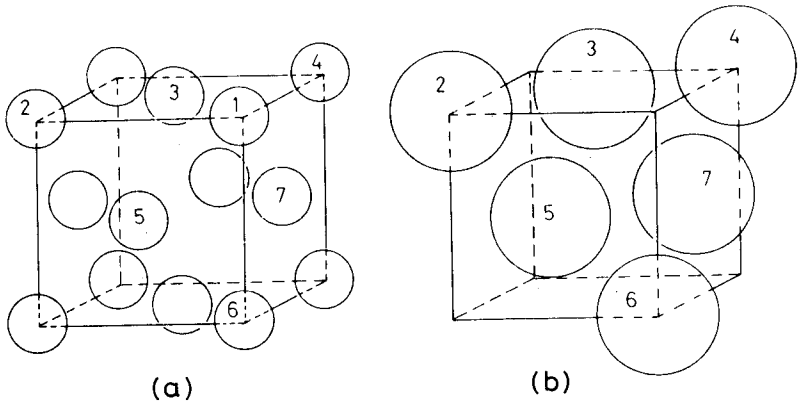

Fig. 7.5 Face centred cubic unit cell of a c.c.p. arrangement of spheres

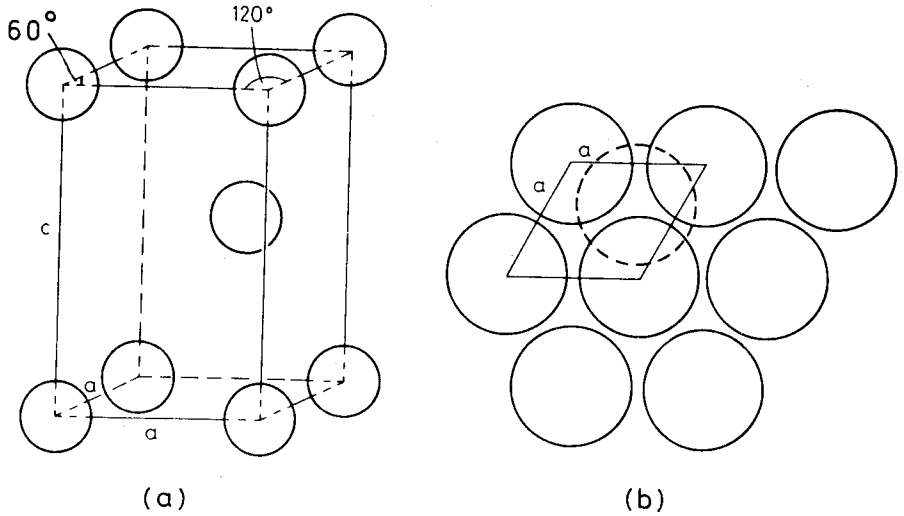

Fig. 7.6 Hexagonal unit cell of an h.c.p. arrangement of spheres

a c.c.p. structure, c.p. layers occur in four orientations perpendicular to the body diagonals of the cube (the cube has eight corners but each layer orientation is then counted twice, giving four different orientations).

The hexagonal unit cell of an h.c.p. arrangement of spheres (Fig. 7.6) is simpler in that the *basal plane* of the cell coincides with a c.p. layer of spheres (b). The unit cell contains only two spheres, one at the origin (and hence at all corners) and one inside the cell at position $\frac{1}{3}, \frac{2}{3}, \frac{1}{2}$ (dashed circle in b). Close packed layers occur in only one orientation in a h.c.p. structure.

In c.p. structures, 74.05 per cent of the total volume is occupied by spheres. This is the maximum density possible in structures constructed of spheres of only one size. This density value may be calculated by considering the volume and contents of unit cells of c.p. structures. In a c.c.p. array of spheres, the unit cell is f.c.c. and contains four spheres, one at a corner and three at face centre positions (Fig. 7.5) (this is equivalent to the statement that a f.c.c. unit cell contains four lattice points).

Close packed directions (XX', YY', ZZ' in Fig. 7.1), in which spheres are in contact, occur parallel to the face diagonals of the unit cell, e.g. spheres 2, 5 and 6 in Fig. 7.5(b) form part of a c.p. row and are parallel to directions of the type ⟨110⟩. If the diameter of a sphere is $2r$, the length of the diagonals is $4r$. The length of the cell edge is then $2\sqrt{2}r$ and the cell volume is $16\sqrt{2}r^3$. The volume of each sphere is $1.33\,\pi r^3$ and so the ratio of the total sphere volume to the unit cell volume is given by:

$$\frac{4 \times 1.33\pi r^3}{16\sqrt{2}\,r^3} = 0.7405$$

Similar results are obtained for hexagonal close packing by considering the contents and volume of the appropriate hexagonal unit cell (Fig. 7.6).

In non-close packed structures, densities lower than 0.7405 are obtained, e.g. the density of body centred cubic (b.c.c.) is 0.6802 (to calculate this it is necessary to know that the c.p. directions in b.c.c. are ⟨111⟩, i.e. parallel to the body diagonals of the cube).

7.1.2 Materials that can be described as close packed structures

7.1.2.1 *Metals*

Most metals crystallize in one of the three arrangements, c.c.p., h.c.p. and b.c.c., the first two of which are c.p. structures. The distribution of structure type among the metals is irregular (Table 7.1 and Appendix 9) and no clear-cut trends are observed. It is still not well understood why particular metals prefer one structure type to another. Calculations reveal that the lattice energies of h.c.p. and c.c.p. metal structures are comparable and, therefore, the structure observed in a particular case probably depends on fine details of the bonding requirements or band structures of the metal.

Some metals are *polymorphic* and exhibit more than one structure type, e.g. iron can be either c.c.p. or b.c.c. depending on temperature, cobalt can be either c.c.p. or h.c.p. but other forms also exist which possess more complex stacking sequences of c.p. layers. *Polytypism* is the name given to a special kind of polymorphism in that the structural differences between *polytypes* are confined to one dimension only. In c.p. metal structures, the arrangement of atoms within one c.p. layer is the same as that in any other c.p. layer and structural differences are confined to the way in which layers are stacked relative to each other. There are two simple stacking sequences, h.c.p., AB, and c.c.p., ABC, but an infinite number of more complex sequences, and some of these larger repeat units are observed in cobalt metal polytypes. In some polytypic materials, very long sequences have been observed which contain several hundred layers in the repeat unit. It is an

Table 7.1 *Structures and unit cell dimensions* (Å) *of some common metals*

Cubic close packed, *a*		Hexagonal close packed, *a*, *c*			Body centred cubic, *a*	
Cu	3.6147	Be	2.2856,	3.5832	Fe	2.8664
Ag	4.0857	Mg	3.2094,	5.2105	Cr	2.8846
Au	4.0783	Zn	2.6649,	4.9468	Mo	3.1469
Al	4.0495	Cd	2.9788,	5.6167	W	3.1650
Ni	3.5240	Ti	2.506,	4.6788	Ta	3.3026
Pd	3.8907	Zr	3.312,	5.1477	Ba	5.019
Pt	3.9239	Ru	2.7058,	4.2816		
Pb	4.9502	Os	2.7353,	4.3191		
		Re	2.760,	4.458		

intriguing question as to how such regular and long range structures form; for instance, after a repeat unit involving several hundred layers and a distance of, say, 500 Å, what kind of forces dictate that this sequence shall be repeated in the next 500 Å? As yet, this has not been explained satisfactorily although it has been suggested that screw dislocations may provide a mechanism of spiral crystal growth which could conceivably lead to these very large repeat units.

Stacking disorder is mentioned in Chapter 9 and occurs quite commonly; in this, pairs of layers in an otherwise regular stacking sequence are reversed, as in:

... ABCABCABCA*CB*ABCABC ...

This is an example of a two-dimensional or planar crystal defect. In some highly disordered materials, random stacking sequences occur.

7.1.2.2 *Alloys*

Alloys are intermetallic phases or solid solutions and, as is the case for pure metals, many can be regarded as c.p. structures. As an example, copper and gold both crystallize in c.c.p. structures and at high temperatures a complete range of *solid solutions* between copper and gold forms. In these the copper and gold atoms are statistically distributed over the lattice points of the f.c.c. unit cell and therefore the c.c.p. layers contain a random mixture of copper and gold atoms. On annealing the alloy compositions AuCu and $AuCu_3$ at lower temperatures, the gold and copper atoms order themselves; c.c.p. layers still occur but the arrangement of gold and copper atoms within the layers is no longer statistical. Order–disorder phenomena are discussed further in Chapter 12.

7.1.2.3 *Ionic structures*

The structures of materials such as NaCl, Al_2O_3, Na_2O, ZnO, etc., in which the anion is somewhat larger than the cation, can be regarded as built of c.p. layers of anions with the cations placed in interstitial sites. A considerable variety of structure types are possible in which the variables are the stacking sequence of the anions, either h.c.p. or c.c.p., and the number and type of interstitial sites that are occupied by cations. Before these structures are considered, some general comments (discussed in more detail in the next chapter) should be made.

In c.p. metallic structures, all the atoms are of one type and it may be assumed that nearest neighbour atoms are in contact. With ionic structures, ions of opposite charge are present and the resulting structure is a balance of attractive and repulsive electrostatic forces. Further, since there are two (at least) types of ion present, their relative sizes affect the structure that is adopted. Although, for many purposes, it is convenient to regard ionic structures such as NaCl as containing c.p. anion layers with cations in interstitial sites, in fact the cations are often too large for the prescribed interstitial sites. The structure can accommodate them only by expanding the anion array. Consequently, the arrangement of anions is the same as in a c.p. array of spheres, but the anions may not be in

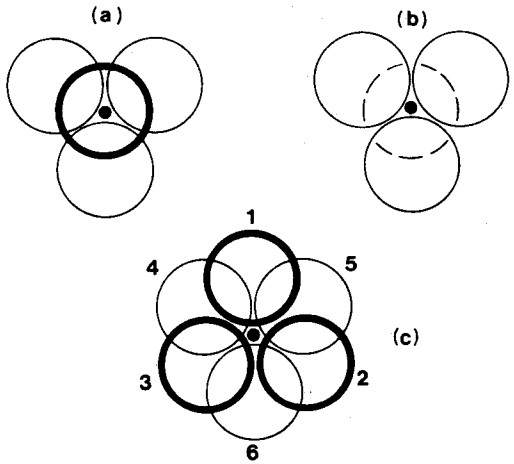

Fig. 7.7 Interstitial sites in a c.p. structure. Heavy circles are above and the dashed circles below the plane of the paper: (a) T_+ site, (b) T_- site, (c) O site

contact. O'Keeffe has suggested the term *eutactic* for structures such as these in which the arrangement of ions is the same as that in a c.p. array but in which the ions are not necessarily contacting. In the subsequent discussion of ionic structures use of the terms h.c.p. and c.c.p. for the anion arrays does not necessarily imply that the anions are in contact but rather that the structures are eutactic.

Two types of interstitial sites, tetrahedral and octahedral, are present in c.p. structures (Fig. 7.7). For the tetrahedral sites, three anions that form the base of the tetrahedron belong to one c.p. layer with the apex of the tetrahedron in the layer above (a) or below (b). This gives two types of tetrahedral site, T_+ and T_-, in which the apex is up and down, respectively. Because the centre of gravity of a tetrahedron is nearer to the base than to the apex (Appendix 1) cations in tetrahedral sites are not located midway between adjacent anion layers but are nearer to one layer than the other. Octahedral sites, on the other hand, are coordinated to three anions in each layer (Fig. 7.7c) and are placed midway between the anion layers. A more common way of regarding octahedral coordination is as four coplanar atoms with one atom at each apex above and below the plane. In (c), atoms 1, 2, 4 and 6 are coplanar; 3 and 5 form apices of the octahedron. Alternatively, atoms 2, 3, 4, 5 and 1, 3, 5, 6 are coplanar.

The distribution of interstitial sites between any two adjacent layers of c.p. anions is shown in Fig. 7.8. Counting up the numbers of each, for every anion there is one octahedral site and two tetrahedral sites, one T_+ and one T_-. It is rare that all the interstitial sites in a c.p. structure are occupied; often one set is fully or partly occupied and the remaining two sets are empty. A selection of c.p. ionic structures, classified according to the anion layer stacking sequence and the occupancy of the interstitial sites, is given in Table 7.2. Individual structures are

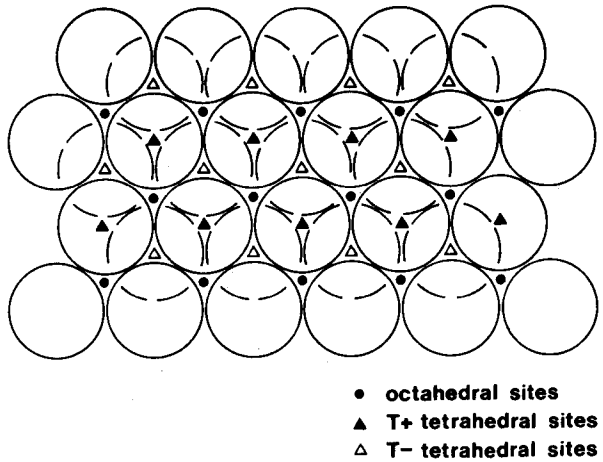

Fig. 7.8 Distribution of interstitial sites between two c.p. layers. Dashed circles are below the plane of the paper

described in more detail later; here we note how a wide range of diverse structures can be grouped into one large family and this helps to bring out the similarities and differences between them. For example:

(a) The rock salt and nickel arsenide structures both have octahedrally coordinated cations and differ only in the anion stacking sequence. A similar relation exists between the structures of olivine and spinel.

Table 7.2 *Some close packed structures*

Anion arrangement	Interstitial sites T_+	T_-	Oct	Examples
c.c.p.	—	—	1	NaCl, rock salt
	1	—	—	ZnS blende or sphalerite
	$\frac{1}{8}$	$\frac{1}{8}$	$\frac{1}{2}$	$MgAl_2O_4$, spinel
	—	—	$\frac{1}{2}$	$CdCl_2$
	1	—	—	$CuFeS_2$
	—	—	$\frac{1}{3}$	$CrCl_3$
	1	1	—	K_2O antifluorite
h.c.p.	—	—	1	NiAs
	1	—	—	ZnS, wurtzite
	—	—	$\frac{1}{2}$	CdI_2
	—	—	$\frac{1}{2}$	TiO_2*, rutile
	—	—	$\frac{2}{3}$	Al_2O_3
	$\frac{1}{8}$	$\frac{1}{8}$	$\frac{1}{2}$	Mg_2SiO_4, olivine
	1	—	—	β-Li_3PO_4
	$\frac{1}{2}$	$\frac{1}{2}$	—	γ-Li_3PO_4*
c.c.p. 'CaO_3' layers	—	—	$\frac{1}{4}$	$CaTiO_3$ perovskite

*The h.c.p. oxide layers in rutile and γ-Li_3PO_4 are not planar but are buckled. The oxide ion arrangement in these may alternatively be described as tetragonal packed (t.p.).

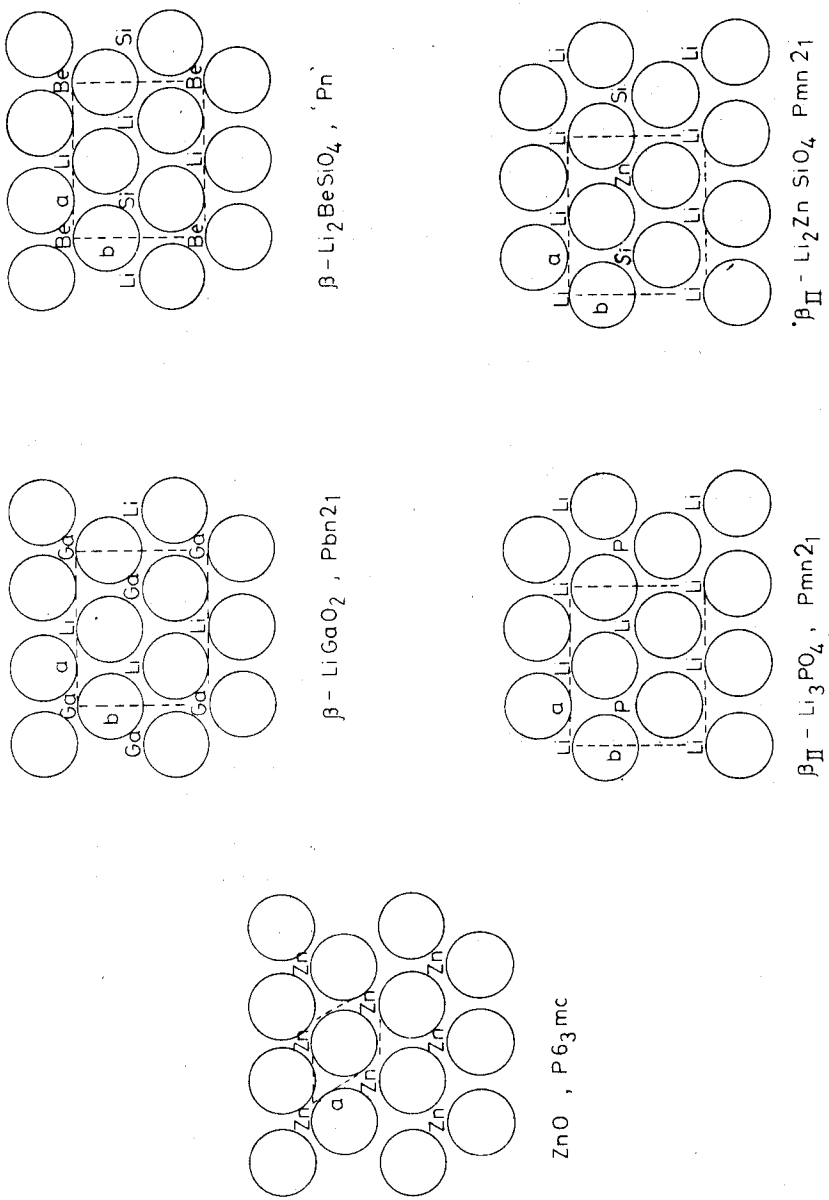

Fig. 7.9 Ordered tetrahedral structures related to the wurtzite structure of ZnO. One oxide layer is shown together with one layer of cations in T_+ tetrahedral sites. Note the different cation ordering sequences. (From West, 1975)

(b) Rutile, TiO_2 and CdI_2 both have hexagonal close packed anions (although the layers are buckled in rutile) with half the octahedral sites occupied by cations but they differ in the manner of occupancy of these octahedral sites. In rutile, half the octahedral sites between any pair of c.p. anion layers are occupied by Ti^{4+}, in ordered fashion; in CdI_2, layers of fully occupied octahedral sites alternate with layers in which all sites are empty and this gives CdI_2 an obvious layered structure which is reflected in its physical properties.

(c) Both β and γ polymorphs of Li_3PO_4 have h.c.p. oxide ions (although the layers are buckled, especially in γ) with half the tetrahedral sites occupied by cations; in β-Li_3PO_4, all the T_+ sites are occupied with T_- sites empty, but in γ-Li_3PO_4 half of both the T_+ and T_- sites are occupied, in ordered fashion.

(d) A large number of more complex c.p. structures are possible. For example, in the series; ZnO, $LiGaO_2$, β-Li_3PO_4, β-Li_2ZnSiO_4, all the compounds have structures related to that of ZnO. The T_+ sites are fully occupied in each but different structures arise as the cations order themselves in different ways over the T_+ sites (Fig. 7.9).

(e) In a few structures, it is useful to regard the *cation* as forming the c.p. layers with the anions occupying the interstitial sites. The most common example is the fluorite structure, CaF_2, which may be regarded as cubic close packed Ca^{2+} ions with all the T_+ and T_- tetrahedral sites occupied by F^- ions. The antifluorite structure of, for example, K_2O is the exact inverse of fluorite and is included in Table 7.2.

(f) The close packing concept may be extended to include structures in which a mixture of anions and large cations form the packing layers and smaller cations occupy the interstitial sites. In perovskite, $CaTiO_3$, c.c.p. layers of composition 'CaO_3' occur and one quarter of the octahedral sites between these layers are occupied by titanium. Some of the octahedral sites must contain Ca^{2+} ions at the corners, but Ti^{4+} occupies those octahedral sites in which all six corners are O^{2-} ions, Fig. 6.15.

(g) Some structures may be regarded as anion-deficient c.p. structures in which the anions form an essentially c.p. array but in which some are missing. The ReO_3 structure may be regarded as having c.c.p. oxide layers with one quarter of the O^{2-} ion sites empty. It is analogous to the perovskite structure just described in which the Ti^{4+} ions are replaced by Re^{6+} and the Ca^{2+} ions are removed and their sites left vacant. The structure of β-alumina, nominally of formula $NaAl_{11}O_{17}$, contains c.p. oxide layers in which every fifth layer has approximately three quarters of the O^{2-} ions missing.

7.1.2.4 *Covalent network structures*

Materials such as diamond and silicon carbide, which have very strong, directional, covalent bonds, can also be described as c.p. structures or eutactic structures; many have the same structures as ionic compounds (Section 7.1.2.3). Thus, one polymorph of SiC has the wurtzite structure and it is immaterial

whether silicon or carbon is regarded as the packing atom since the net result—a three-dimensional framework of corner sharing tetrahedra—is the same. Diamond can be regarded as a sphalerite structure in which half the carbon atoms form a c.c.p. array and the other half occupy T_+ interstitial sites, but again the two types of atom are equivalent. Classification of diamond as a eutactic structure is useful since in diamond all the atoms are of the same size and it is unrealistic to distinguish between packing atoms and interstitial atoms.

Many structures have mixed ionic–covalent bonding, e.g. ZnS and $CrCl_3$ in Table 7.2, and one advantage of describing their structures in terms of close packing is that this can be done, if necessary, without reference to the type of bonding that is present.

7.1.2.5 *Molecular structures*

Since c.p. structures provide an efficient means of packing atoms together, many molecular compounds crystallize as c.p. structures even though the bonding forces between adjacent molecules are weak van der Waals forces. If the molecules are roughly spherical in shape or become spherical because they can rotate or occupy different orientations at random, then simple h.c.p. or c.c.p. structures result, e.g. in crystalline H_2, CH_4 and HCl. Non-spherical molecules,

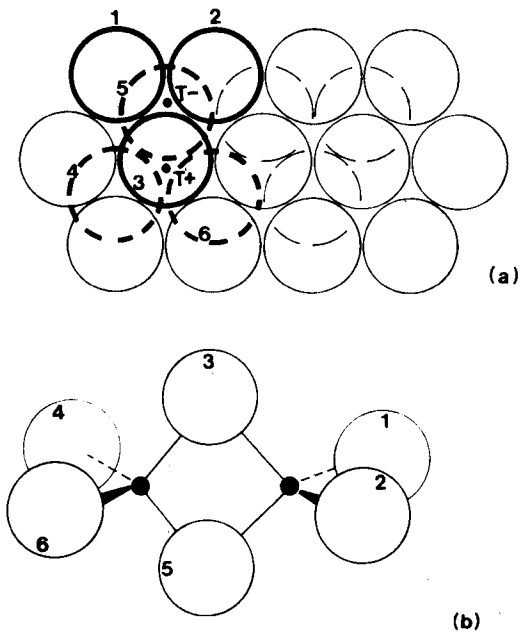

Fig. 7.10 Hexagonal close packing arrangement of bromine atoms in crystalline Al_2Br_6 molecules; aluminium atoms occupy T_+ and T_- sites. Dashed circles are below the plane of the paper

especially if they are built of tetrahedra and octahedra, can also fit into a c.p. arrangement. For example, Al_2Br_6 is a dimeric molecule which can be regarded as two $AlBr_4$ tetrahedra sharing a common edge (Fig. 7.10b). In crystalline Al_2Br_6, the bromine atoms form an h.c.p. arrangement and aluminium atoms occupy $\frac{1}{6}$ of the available tetrahedral sites. One molecule, with the bromine atoms in heavy outline is shown in Fig. 7.10(a); aluminium atoms occupy one pair of adjacent T_+ and T_- sites. Bromine atoms 3 and 5 are common to both tetrahedra and are the bridging atoms in (b). Adjacent Al_2Br_6 molecules are arranged so that each bromine in the h.c.p. array belongs to only one molecule. $SnBr_4$ is a tetrahedral molecule and also crystallizes with an h.c.p. bromine array but now only one eighth of the tetrahedral sites are occupied.

7.1.3 Other packing arrangements: tetragonal packing

The two c.p. arrangements, h.c.p. and c.c.p., are the most efficient ways of packing spheres in three dimensions. They are characterized by a coordination number of 12 and a density of 74.05 per cent. Only slightly less dense is the *primitive tetragonal packed* (p.t.p.) arrangement with a coordination number of 11 and a packing density of 71.87 per cent, and the *body centred tetragonal* (b.c.t.) arrangement with a coordination number of 10 and a packing density of 69.81 per cent. Although the p.t.p. arrangement has been discovered only recently, it is, in fact, commonly occurring and forms the basis of the anion array in structures such as rutile, TiO_2, ramsellite, MnO_2, and γ tetrahedral structures such as γ-Li_3PO_4 and γ-$LiAlO_2$.

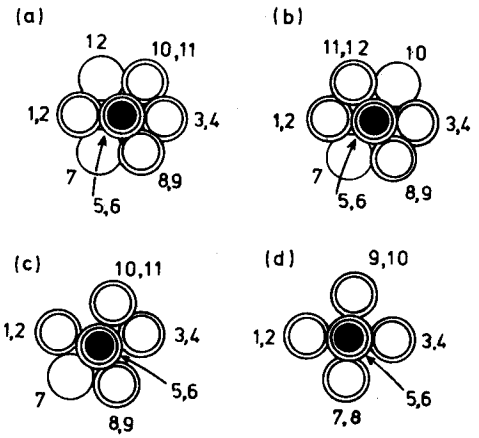

Fig. 7.11 Coordination number of shaded atom of (a) 12 in h.c.p., (b) 12 in c.c.p., (c) 11 in primitive tetragonal packing (p.t.p.) and (d) 10 in body centred tetragonal (b.c.t.). It is found that (c) occurs in various structures including rutile, TiO_2, ramsdellite, MnO_2, and γ tetrahedral oxides, γ-$LiAlO_2$, γ-Li_3PO_4. (From West and Bruce, 1982)

The coordination number and environment in p.t.p. and b.c.t. are shown in Fig. 7.11, together with those for h.c.p. and c.c.p. The p.t.p. arrangement (Fig. 7.11c) may be regarded as derived from h.c.p. in that sphere 12 in Fig. 7.11(a) is no longer part of the coordination sphere of the shaded atom in Fig. 7.11(c) and atoms 1 to 6, which together with the shaded atom are coplanar in Fig. 7.11(a), are slightly non-coplanar in Fig. 7.11(c). A more extended version of Fig. 7.11(c) can be seen in Fig. 6.16(d) which shows the oxide ion arrangement in rutile.

The interstitial sites in a p.t.p. array fall into two categories: (a) tetrahedral and octahedral sites that are undistorted, as in h.c.p.; (b) tetrahedral and octahedral sites that are distorted. The undistorted sites can be occupied by a variety of cations, e.g. octahedral sites are occupied by Ti(TiO_2), Mn(MnO_2) and tetrahedral sites by Li, Al($LiAlO_2$), Li, P(Li_3PO_4). The distorted sites, on the other hand, are usually empty.

The b.c.t. arrangement (Fig. 7.11d) appears not to occur in known crystal structures. This may be because it does not have undistorted interstitial sites suitable for occupation by cations.

7.1.4 Structures built of space filling polyhedra

This approach to describing crystal structures emphasizes the coordination number of the cations and the way that structures may be regarded as built of polyhedra linked together by sharing corners, edges or faces. For example, in NaCl, each Na^+ ion has six Cl^- ions as its nearest neighbours, arranged octahedrally; this is represented as an octahedron with Cl^- ions at the corners and Na^+ at the centre. A three-dimensional overview of the structure is obtained by looking at the way in which neighbouring octahedra are linked to each other. In NaCl, each octahedron edge is shared between two octahedra, resulting in an infinite framework of edge-sharing octahedra. Although the polyhedra may link up to form a three-dimensional framework, not all the available space is usually filled; e.g. in NaCl, empty tetrahedral cavities remain within the framework of octahedra. These cavities are shown in Appendix 2 for a single layer of octahedra. Also shown in the Appendix are pictures of various polyhedral linkages and hints on making one's own models from card paper are given.

Although it is legitimate to estimate the efficiency of packing of spheres in c.p. structures, it is incorrect to do this for space filling polyhedra since the anions, usually the largest ions in the structure, are represented by points at the corners of the polyhedra. In spite of this obvious misrepresentation, the space filling polyhedron approach has the advantage that it shows the topology or connectivity of a framework structure and indicates clearly the location of empty interstitial sites. Some examples of structures that can be viewed as built of space filling polyhedra are given in Table 7.3. A variety of polyhedra occur in inorganic structures, although tetrahedra and octahedra appear to be the most common.

A complete scheme for classifying polyhedral structures has been proposed by Wells and others in which the initial problem is a geometrical one—what types of network built of linked polyhedra are possible? The variables to be considered

Table 7.3 *Some structures built of space filling polyhedra*

Octahedra only	
12 edges shared	NaCl
6 corners shared	ReO_3
3 edges shared	$CrCl_3$, BiI_3
2 edges and 6 corners shared	TiO_2
4 corners shared	$KAlF_4$
Tetrahedra only	
4 corners shared (between 4 tetrahedra)	ZnS
4 corners shared (between 2 tetrahedra)	SiO_2
1 corner shared (between 2 tetrahedra)	$Si_2O_7^{6-}$
2 corners shared (between 2 tetrahedra)	$(SiO_3)_n^{2n-}$, chains or rings

are the following. Polyhedra may share some or all of their corners, edges and faces with adjacent polyhedra, which may or may not be of the same type. The corners and edges may be common to more than two polyhedra (obviously, only two polyhedra can share a common face); e.g. in SiO_2, each corner (oxygen) is shared between two (SiO_4) tetrahedra but in ZnS each corner is shared between four tetrahedra; in spinel, $MgAl_2O_4$, each corner is shared between three octahedra and one tetrahedron. An enormous number of structures are feasible, at least theoretically, and it is an interesting exercise to categorize real structures on this basis.

This classification scheme for non-metallic materials has not, as yet, received a wide acceptance, perhaps because by its very nature it is all-embracing and indicates similarities between different structures whereas physically or chemically perhaps none exists. The topological problem of what kinds of structure may be generated by arranging polyhedra in various ways takes no account of the bonding forces between atoms or ions. Such information must come from elsewhere. Also the description of structures in terms of polyhedra does not necessarily imply that such entities exist in the structure as separate species. Thus, in NaCl, the bonding is mainly ionic and physically distinct $NaCl_6$ octahedra do not occur. Similarly, SiC has a covalent network structure and separate SiC_4 tetrahedral entities do not exist. Polyhedra *do* have a separate existence in structures of (a) molecular materials, e.g. Al_2Br_6 contains pairs of edge-sharing tetrahedra, and (b) compounds that contain complex ions, e.g. the silicate structures are built up of SiO_4 tetrahedra which link up to form complex anions ranging in size from isolated monomeric units to infinite chains and sheets and, finally, three-dimensional frameworks.

In considering the types of polyhedral linkage that are likely to occur in crystal structures, Pauling's third rule for the structures of complex ionic crystals (next chapter) provides a very useful guideline. This rule states that the presence of shared polyhedron edges and, especially, shared faces decreases the stability of a structure. The effect is particularly large for cations of high valence and small

coordination number, i.e. for small polyhedra, especially tetrahedra, that contain highly charged cations. When polyhedra share edges and, particularly, faces, the cation–cation distances (i.e. the distances between the centres of the polyhedra) decrease and the cations repel each other electrostatically. In Fig. 7.12 are shown pairs of (a) corner-sharing and (b) edge-sharing octahedra. The cation–cation distance is clearly less in the latter and for face-sharing octahedra, not shown, the cations are even closer. Comparing edge-shared tetrahedra and edge-shared octahedra, the cation–cation distance M–M (relative to the cation–anion distance M–X) is less between the edge-shared tetrahedra because the MXM bridging angle is (c) 71° for the tetrahedra and (b) 90° for the octahedra. A similar effect occurs for face-sharing tetrahedra and octahedra. In Table 7.4, the M–M distances for the various polyhedral linkages are given as a function of the distance M–X. The M–M distance is greatest for corner sharing of either tetrahedra or octahedra and is least for face-sharing tetrahedra. For the sharing of corners and edges, the M–M distances given are the maximum possible distances. Reduced distances occur if the polyhedra are rotated about the shared corner or edge (e.g. so that the M–X–M angle between corner-shared polyhedra is less than 180°).

From Table 7.4, the M–M distance in face-shared tetrahedra is considerably less than the M–X bond distance. This represents an unstable situation, therefore,

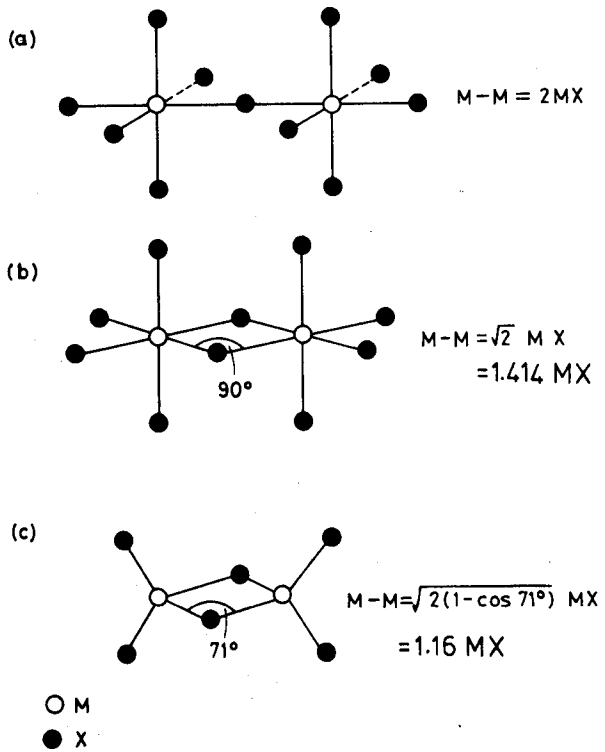

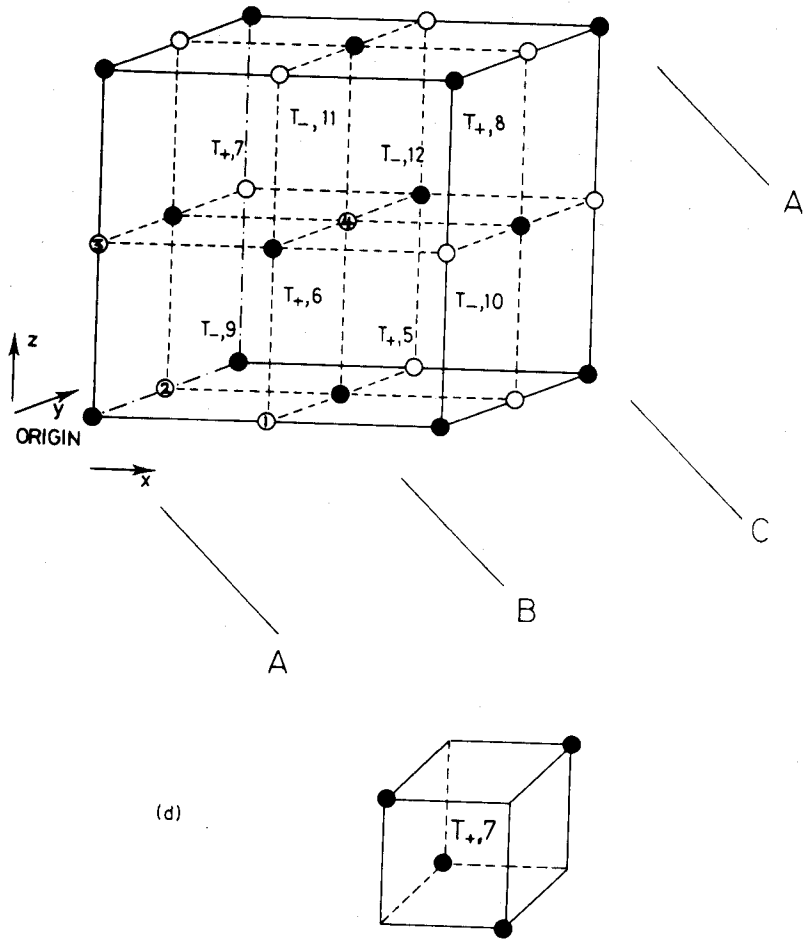

Fig. 7.12 Cation–cation separation in octahedra which share (a) corners and (b) edges and in tetrahedra which (c) share edges. (d) Available cation sites in an f.c.c. anion array

Table 7.4 *The distance M–M between centres of regular MX_4 or MX_6 groups sharing X atom(s).* (Data taken from Wells, 1975)

	Sharing a common		
	corner*	edge*	face
Two tetrahedra	2.00 MX(tet.)	1.16 MX(tet.)	0.67 MX(tet.)
Two octahedra	2.00 MX(oct.)	1.41 MX(oct.)	1.16 MX(oct.)

*Maximum possible value.

because of the large cation–cation repulsions which would arise, and does not normally occur. A good example is provided by the absence of any crystal whose structure is the h.c.p. equivalent of the fluorite (or antifluorite) structure. In, for example, Na_2O which has the antifluorite structure, the oxide ions are in a c.c.p. array and the NaO_4 tetrahedra share edges. However, in a structure with an h.c.p. anion array and all the tetrahedral cation sites occupied, the MX_4 tetrahedra would share faces. Edge sharing of tetrahedra in which the M–M separation is only 16 per cent larger than the M–X bond distance appears to be energetically acceptable in principle, as shown by the common occurrence of compounds with a fluorite type of structure, but face sharing of tetrahedra is unacceptable.

For tetrahedra containing cations of high charge, edge sharing appears to be unacceptable and only corner sharing occurs. Thus, in silicate structures, which are built of SiO_4 tetrahedra, edge sharing of SiO_4 tetrahedra never occurs*. In an ideally ionic structure the charge on silicon would be 4+, but the actual charges are considerably less due to partial covalency of the Si—O bonds.

An additional factor to be taken into account when comparing linkages of tetrahedra and octahedra (Table 7.4) is that, for a given M and X, the M–X distance varies, depending on the nature of the polyhedra. In a c.p. structure, the tetrahedral sites are smaller than the octahedral sites, i.e.

$$\frac{\text{M–X in MX}_4\text{(tet.)}}{\text{M–X in MX}_6\text{(oct.)}} = \frac{\sqrt{3}}{2} = 0.866$$

This may be shown by, for example, calculating and comparing the M–X distances present in the f.c.c. cells of NaCl and CaF_2 structures (see Table 7.8).

7.2 Some important structure types

7.2.1 Rock salt (NaCl), zinc blende or sphalerite (ZnS) and antifluorite (Na_2O)

These structures are considered together because they have in common a cubic close packed (i.e. a face centred cubic) arrangement of anions and differ only in the positions of the cations. In Fig. 7.12(d) are shown the anions (●) in a f.c.c. unit cell with octahedral O, tetrahedral T_+ and tetrahedral T_- sites for the cations. Octahedral sites occur at the edge centre 1, 2, 3 and body centre 4 positions. In order to see the T_+ and T_- sites clearly it is convenient to divide the unit cell into eight smaller cubes by bisecting each cell edge (dashed lines). These smaller cubes contain anions at only four of the eight corners and in the middle of each small cube is a tetrahedral site (inset, Fig. 7.12d). Note that this is a useful way to represent tetrahedra and permits ready calculation of bond distances, bond angles, etc., in tetrahedra. A tetrahedral site occurs in the middle of each smaller cube and parallel to any of the cell axes, x, y and z, T_+ and T_- sites alternate.

*By contrast, in SiS_2, edge sharing of SiS_4 tetrahedra occurs. The Si—S bond is longer than and more covalent than the Si—O bond and both effects act to reduce the Si—Si repulsion; consequently edge sharing becomes acceptable.

The c.p. anion layers are oriented parallel to the {111} planes of the unit cell (Fig. 7.5) and four such layers, ABCA, are indicated in Fig. 7.12(d). The coordinates of the anions in the unit cell (Chapter 6) are

$$000, \quad \tfrac{1}{2}\tfrac{1}{2}0, \quad \tfrac{1}{2}0\tfrac{1}{2}, \quad 0\tfrac{1}{2}\tfrac{1}{2}$$

Only one corner atom is included in this list, at 000, since the other seven corner atoms, at 100, 110, etc., are equivalent and can be regarded as the corner atoms of adjacent unit cells. Likewise for each pair of opposite faces, e.g. $\tfrac{1}{2}\tfrac{1}{2}0$ and $\tfrac{1}{2}\tfrac{1}{2}1$, only one of these is specified since the other is equivalent and is generated by translation of one unit cell dimension in the z direction.

The various cation positions have the following coordinates:

Octahedral:	$1-\tfrac{1}{2}00$,	$2-0\tfrac{1}{2}0$,	$3-00\tfrac{1}{2}$,	$4-\tfrac{1}{2}\tfrac{1}{2}\tfrac{1}{2}$
Tetrahedral T_+:	$5-\tfrac{3}{4}\tfrac{1}{4}\tfrac{1}{4}$,	$6-\tfrac{1}{4}\tfrac{3}{4}\tfrac{1}{4}$,	$7-\tfrac{1}{4}\tfrac{1}{4}\tfrac{3}{4}$,	$8-\tfrac{3}{4}\tfrac{3}{4}\tfrac{3}{4}$
Tetrahedral T_-:	$9-\tfrac{1}{4}\tfrac{1}{4}\tfrac{1}{4}$,	$10-\tfrac{3}{4}\tfrac{3}{4}\tfrac{1}{4}$,	$11-\tfrac{1}{4}\tfrac{3}{4}\tfrac{3}{4}$,	$12-\tfrac{3}{4}\tfrac{1}{4}\tfrac{3}{4}$

Note that there are four of each type of cation site, O, T_+, T_-, in the unit cell together with four anions. By having different sites occupied, different structures are generated, as follows:

Rock salt: O sites occupied by cations; T_+, T_- empty

Zinc blende: T_+ (or T_-) sites occupied; O, T_- (or T_+) empty

Antifluorite: T_+, T_- occupied; O empty.

Unit cells of these three structures are shown in Fig. 7.13(a), (b) and (c). In Fig. 7.13(d), (e) and (f), the structures are shown in the same orientation but now the coordination numbers of the ions are emphasized. In rock salt (d), both anions and cations are octahedrally coordinated, whereas in zinc blende (e) both are tetrahedrally coordinated. In antifluorite (f), cations are tetrahedrally coordinated and anions are eight-coordinated (not shown).

A general rule regarding coordination numbers is that in any structure of formula A_xX_y, the coordination numbers of A and X must be in the ratio of y:x. In both rock salt and zinc blende, $x = y$ and therefore, in each, anions and cations have the same coordination number. In antifluorite, of formula A_2X, the coordination numbers of cation and anion must be in the ratio of 1:2. Since the cations occupy tetrahedral sites, the anion coordination number must therefore be eight.

The tetrahedral cation coordination in antifluorite is shown in 7.13(f). In order to see the anion coordination number of eight, it is convenient to redefine the origin of the unit cell so that the origin coincides with a cation rather than an anion. This may be done by displacing the unit cell along one of the body diagonals and by one quarter of the length of the diagonal. The cation at X in (c), with coordinates $\tfrac{1}{4}\tfrac{1}{4}\tfrac{1}{4}$, may be chosen as the new origin of the unit cell. The coordinates of the atoms in the new cell are given by subtracting $\tfrac{1}{4}\tfrac{1}{4}\tfrac{1}{4}$ from their coordinates in the old cell, i.e.

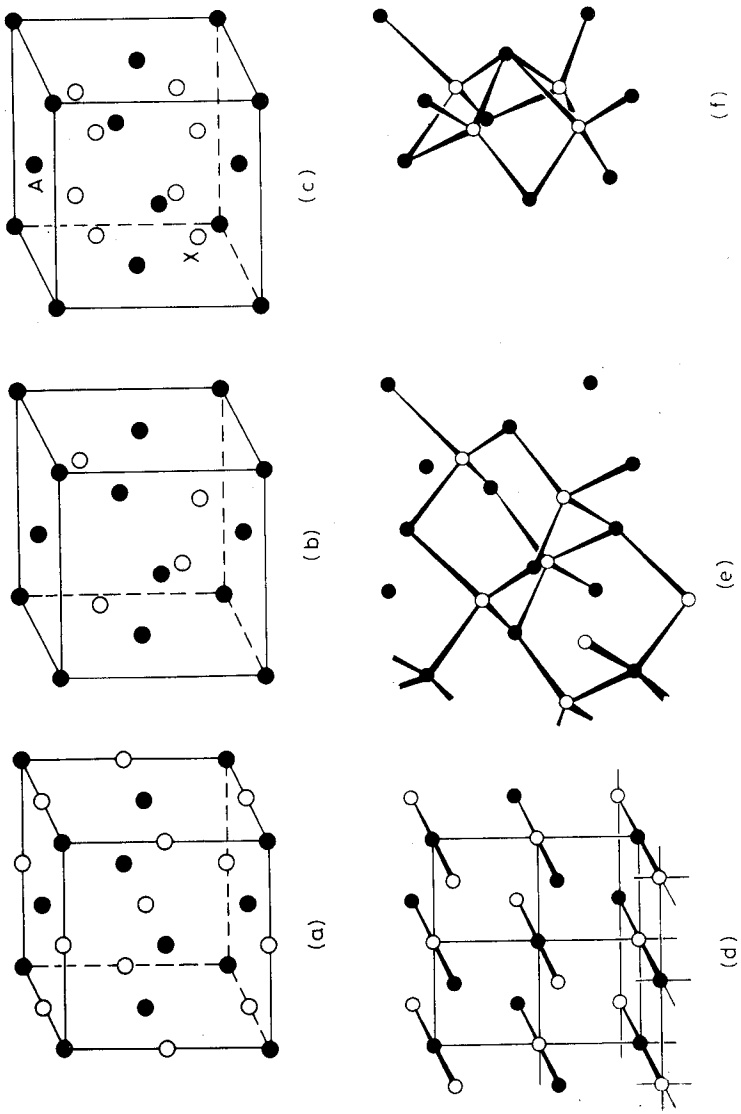

Fig. 7.13 Unit cell of (a) NaCl, (b) ZnS, sphalerite, and (c) Na_2O. Open circles are cations; closed circles anions. Coordination numbers of ions in (d) NaCl, (e) ZnS and (f) Na_2O

	Old cell	New cell
Anions	000	$-\frac{1}{4}-\frac{1}{4}-\frac{1}{4}\rightarrow\frac{3}{4}\frac{3}{4}\frac{3}{4}$
	$\frac{1}{2}\frac{1}{2}0$	$\frac{1}{4}\ \frac{1}{4}-\frac{1}{4}\rightarrow\frac{1}{4}\frac{1}{4}\frac{3}{4}$
	$\frac{1}{2}0\frac{1}{2}$	$\frac{1}{4}-\frac{1}{4}\ \frac{1}{4}\rightarrow\frac{1}{4}\frac{3}{4}\frac{1}{4}$
	$0\frac{1}{2}\frac{1}{2}$	$-\frac{1}{4}\ \frac{1}{4}\ \frac{1}{4}\rightarrow\frac{3}{4}\frac{1}{4}\frac{1}{4}$
Cations	$\frac{1}{4}\frac{1}{4}\frac{1}{4}$	0 0 0
	$\frac{1}{4}\frac{1}{4}\frac{3}{4}$	0 0 $\frac{1}{2}$
	$\frac{1}{4}\frac{3}{4}\frac{1}{4}$	0 $\frac{1}{2}$ 0
	$\frac{3}{4}\frac{1}{4}\frac{1}{4}$	$\frac{1}{2}$ 0 0
	$\frac{1}{4}\frac{3}{4}\frac{3}{4}$	0 $\frac{1}{2}$ $\frac{1}{2}$
	$\frac{3}{4}\frac{1}{4}\frac{3}{4}$	$\frac{1}{2}$ 0 $\frac{1}{2}$
	$\frac{3}{4}\frac{3}{4}\frac{1}{4}$	$\frac{1}{2}$ $\frac{1}{2}$ 0
	$\frac{3}{4}\frac{3}{4}\frac{3}{4}$	$\frac{1}{2}$ $\frac{1}{2}$ $\frac{1}{2}$

In cases where negative coordinates occur as a result of this subtraction, e.g. $-\frac{1}{4}-\frac{1}{4}-\frac{1}{4}$, the position lies outside the new unit cell and it is necessary to find an equivalent position within the unit cell. In this particular case, one is added to each coordinate, giving $\frac{3}{4}\frac{3}{4}\frac{3}{4}$. Addition of one to, say, the x coordinate is equivalent to moving to a similar position in the next unit cell in the x direction. This is illustrated further in Appendix 4. The new unit cell of the antifluorite structure with its origin at cation X, is shown in Fig. 7.14(a). It contains cations at corners, edge centres, face centres and body centre. In order to see the anion coordination more clearly, the unit cell may be imagined as divided into eight smaller cubes (as in Fig. 7.12). Each of these smaller cubes has cations at all eight corners and hence at the centre of each is an eight-coordinate site. Anions occupy four of these eight smaller cubes such that parallel to the cell axes the eight

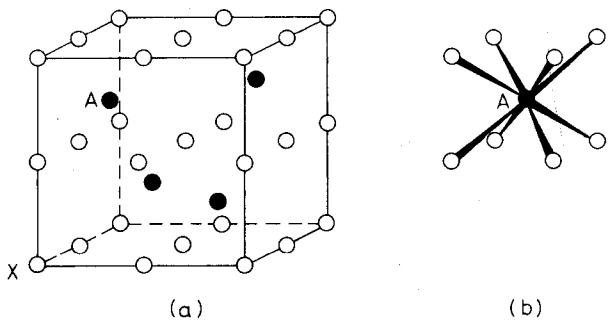

Fig. 7.14 Alternative view of the fluorite and antifluorite structures

coordinate sites are alternately occupied and empty. The eight fold coordination for one anion, A, is shown in Fig. 7.14(b).

In the antifluorite structure, the effect of changing the origin from an anion position to a cation position is to show the structure in a completely different light. This does not happen with the rock salt and zinc blende structures, however. In these the cation and anion positions are interchangeable and it is immaterial whether the origin coincides with an anion or a cation.

So far the NaCl, ZnS and Na_2O structures have been described in two ways: (a) as c.p. structures and (b) in terms of their unit cells. A third way is to regard them as built of space filling polyhedra. In Fig. 7.13(d), (e) and (f) and Fig. 7.14(b), the coordination environment of each ion is shown. Each ion and its nearest neighbours may be represented by the appropriate polyhedron, e.g. a tetrahedron represents a zinc ion and its four sulphide neighbours (or vice versa) in zinc blende. It is then necessary to consider how neighbouring polyhedra are linked—whether by sharing corners, edges or faces.

In the rock salt structure, $NaCl_6$ octahedra share common edges. Each octahedron has twelve edges and each edge is shared between two octahedra. In Fig. 7.15, the unit cell of NaCl is outlined (dotted) and is in the same orientation as in Fig. 7.13(a). Octahedra centred on sodium ions in edge centre positions 1, 2 and 3 are outlined. Octahedra 1 and 2 share a common edge, indicated by the thick dashed line, and octahedra 2 and 3 share a common edge, shown by the thick solid line. Since each octahedron is linked by its edges to twelve other octahedra it is difficult to represent this satisfactorily in a drawing.

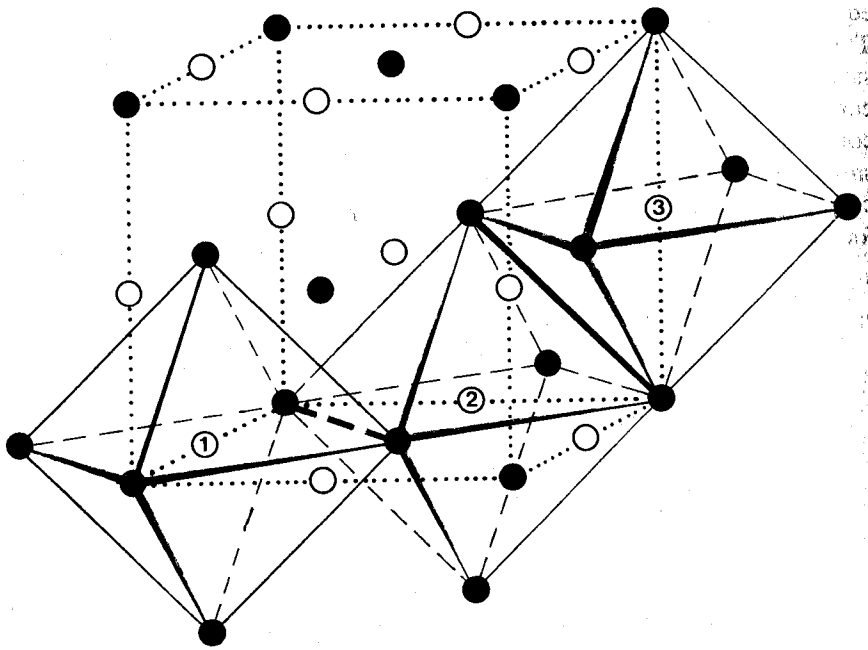

Fig. 7.15 Unit cell of the rock salt structure showing edge sharing of octahedra

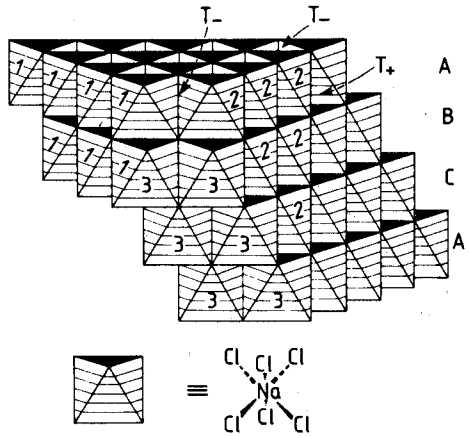

Fig. 7.16 The rock salt structure depicted as an array of edge-sharing octahedra

A schematic drawing showing the rock salt structure as an array of octahedra is shown in Fig. 7.16. Also shown are tetrahedral interstices (arrowed) which are normally empty in NaCl. In this structure, each octahedron face is parallel to layers of c.p. anions. This is emphasized in the drawing in that coplanar octahedron faces are numbered or shaded. Parts of four different sets of faces are shown, corresponding to the four c.p. orientations in a.c.c.p. array.

A large number of AB compounds possess the rock salt structure. A selection is given in Table 7.5 together with values of the *a* dimension of the cubic unit cell. Most halides and hydrides of the alkali metals and Ag^+ have this structure, as do also a large number of the chalcogenides (oxides, sulphides, etc.) of divalent metals such as alkaline earths and divalent transition metals. Many of these are ionic but others, e.g. TiO, have a metallic character.

Table 7.5 *Some compounds with the NaCl structure*

	a(Å)		a(Å)		a(Å)		a(Å)
MgO	4.213	MgS	5.200	LiF	4.0270	KF	5.347
CaO	4.8105	CaS	5.6948	LiCl	5.1396	KCl	6.2931
SrO	5.160	SrS	6.020	LiBr	5.5013	KBr	6.5966
BaO	5.539	BaS	6.386	LiI	6.00	KI	7.0655
TiO	4.177	αMnS	5.224	LiH	4.083	RbF	5.6516
MnO	4.445	MgSe	5.462	NaF	4.64	RbCl	6.5810
FeO	4.307	CaSe	5.924	NaCl	5.6402	RbBr	6.889
CoO	4.260	SrSe	6.246	NaBr	5.9772	RbI	7.342
NiO	4.1769	BaSe	6.600	NaI	6.473	AgF	4.92
CdO	4.6953	CaTe	6.356	NaH	4.890	AgCl	5.549
SnAs	5.7248	SrTe	6.660	ScN	4.44	AgBr	5.7745
TiC	4.3285	BaTe	7.00	TiN	4.240	CsF	6.014
UC	4.955	LaN	5.30	UN	4.890		

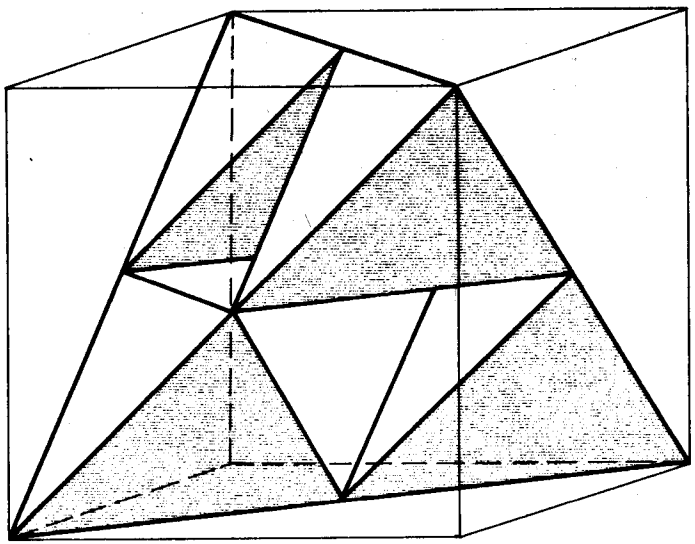

(a)

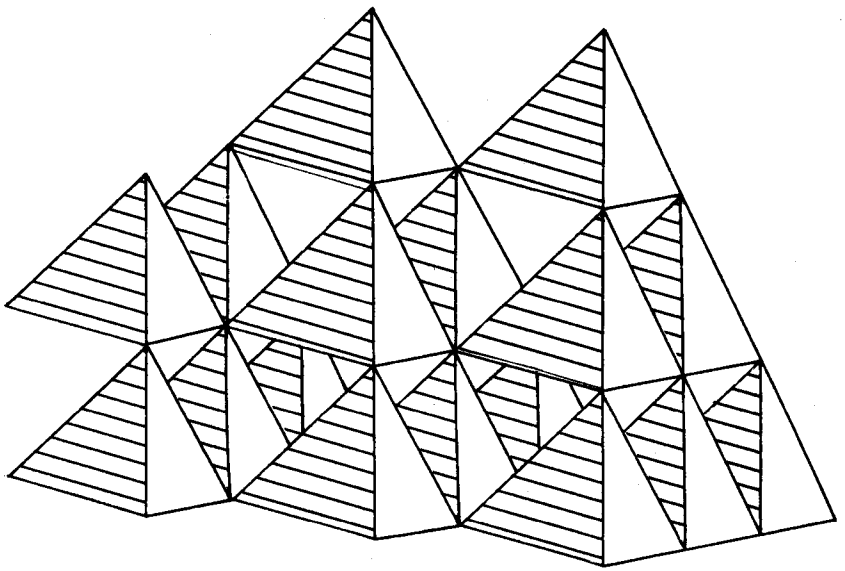

(b)

Fig. 7.17 The sphalerite (zinc blende) structure showing (a) the unit cell contents and (b) a more extended network of corner-sharing tetrahedra

Table 7.6 *Some compounds with the zinc blende (sphalerite) structure*

	a(Å)		*a*(Å)		*a*(Å)		*a*(Å)
CuF	4.255	BeS	4.8624	β-CdS	5.818	BN	3.616	GaP	5.448
CuCl	5.416	BeSe	5.07	CdSe	6.077	BP	4.538	GaAs	5.6534
γ-CuBr	5.6905	BeTe	5.54	CdTe	6.481	BAs	4.777	GaSb	6.095
γ-CuI	6.051	β-ZnS	5.4060	HgS	5.8517	AlP	5.451	InP	5.869
γ-AgI	6.495	ZnSe	5.667	HgSe	6.085	AlAs	5.662	InAs	6.058
β-MnS, red	5.600	ZnTe	6.1026	HgTe	6.453	AlSb	6.1347	InSb	6.4782
β-MnSe	5.88	β-SiC	4.358						

The zinc blende structure contains ZnS_4 tetrahedra or SZn_4 tetrahedra, which are linked at their corners (Fig. 7.13e). Each corner is common to four such tetrahedra; this must be so since anion and cation have the same coordination number in ZnS. The unit cell of zinc blende (Fig. 7.13b and e) is shown again in Fig. 7.17(a), but in terms of corner-sharing ZnS_4 tetrahedra. The faces of the tetrahedra are parallel to the c.p. anion layers, i.e. the {111} planes, and this is emphasized in a more extensive model of the structure (Fig. 7.17b), in which the model is oriented so that one set of tetrahedron faces is approximately horizontal.

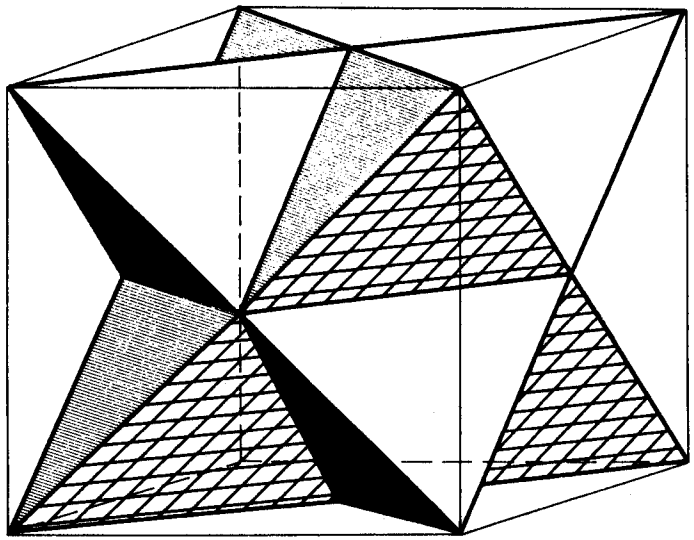

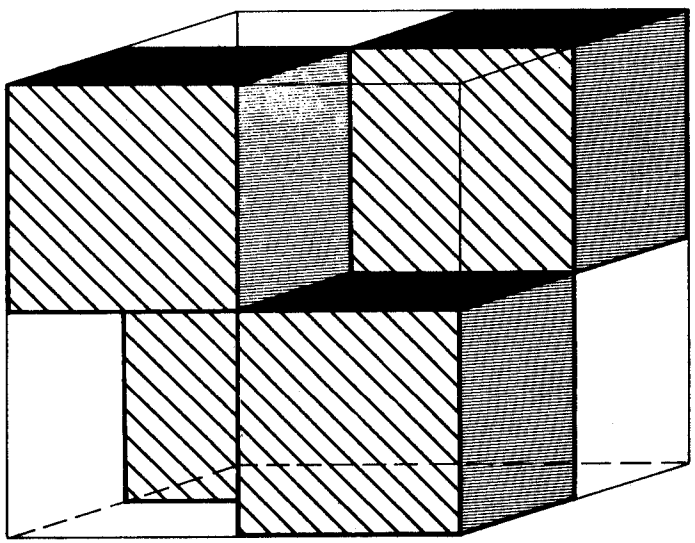

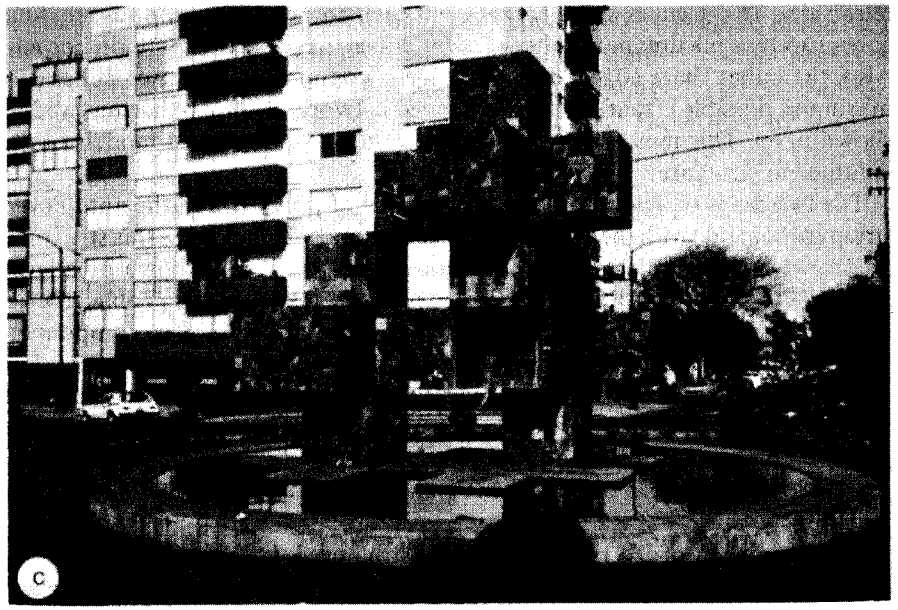

Fig. 7.18 The antifluorite structure showing the unit cell in terms of (a) NaO_4 tetrahedra or (b) ONa_8 cubes. A more extended array of cubes is shown in (c); This model resides on a roundabout in Mexico City

Conventionally, the ZnS structure is regarded as built of c.p. layers of sulphide anions with the smaller zinc cations in tetrahedral sites. Since the same structure is generated by interchanging the Zn^{2+} and S^{2-} ions, the structure could also be described as a c.p. array of Zn^{2+} ions with S^{2-} ions occuping one set of tetrahedral sites. A third, equivalent description is as an array of c.c.p. ZnS_4 (or SZn_4) tetrahedra.

Some compounds which exhibit the zinc blende structure are listed in Table 7.6 together with their cubic lattice parameter, *a*. The bonding in these compounds is less ionic than in corresponding AB compounds which have the rock salt structure. Thus, oxides do not usually have the zinc blende structure (ZnO, not included in Table 7.6, is an exception; it is dimorphic with zinc blende and wurtzite structure polymorphs). Chalcogenides (S, Se, Te) of the alkaline earth metals have the rock salt structure whereas the more covalent corresponding compounds of Be, Zn, Cd and Hg have the zinc blende structure. Most metal(I) halides are like rock salt, with the exception of the more covalent copper(I) halides and γ-AgI.

The antifluorite structure contains tetrahedrally coordinated cations and eight-coordinate anions (Figs 7.13f and 7.14). This leads to two ways of describing the structure, either as a three-dimensional network of tetrahedra or as a three-dimensional network of cubes. The results of these two methods are shown in Fig. 7.18. The unit cell contains either (a) eight NaO_4 tetrahedra or (b) four ONa_8 cubes. In (a), tetrahedra share edges and each edge is common to two

tetrahedra. In (b), cubes share corners, but each corner is common to only four cubes (up to a maximum number of eight cubes may share a common corner). Also, the cubes share edges, but each edge is common to only two cubes (the maximum possible is four). A more extended network of corner-sharing cubes is shown in (c). This must surely rate as one of the world's largest models of the antifluorite structure!

The two ways of describing the arrangement of polyhedra in the antifluorite structure coincide with the two classes of compound which possess this structure. So far, we have considered the *antifluorite* structure which is shown by a large number of oxides and other chalcogenides of the alkali metals (Table 7.7), i.e. compounds of the general formula $A_2^+X^{2-}$. A second group of compounds, which includes fluorides of large, divalent cations and oxides of large tetravalent cations, has the inverse, *fluorite* structure, i.e. $M^{2+}F_2$ and $M^{4+}O_2$. In the fluorite structure, the cations are eight coordinate and the anions are four coordinate, which is the inverse of the antifluorite structure. The arrangement of cubes in Fig. 7.18(b) and (c) also show the MF_8 and MO_8 coordination in the fluorite structure.

A common way of describing the fluorite structure is as a primitive cubic array of anions in which the eight-coordinate sites at the cube body centres are alternately empty and occupied by a cation: this description is consistent with (b) and (c). It should be stressed, however, that the true lattice type of the fluorite structure is face centred cubic and not primitive cubic, since the primitive cubes represent only a small part (one eighth) of the f.c.c. unit cell. Description of the fluorite structure as a primitive cubic array of anions with alternate cube body centres occupied by cations shows a similarity to the CsCl structure (next section). This also has a primitive cubic array of anions, but, instead, cations occupy all the cube body centre sites.

It is very often desirable to be able to make calculations of bond and other interatomic distances in crystal structures. This is usually a straighforward exercise, especially for crystals which have orthogonal unit cells (i.e. $\alpha = \beta =$

Table 7.7 *Some compounds with fluorite and antifluorite structure*

Fluorite structure				Antifluorite structure			
	a(Å)		a(Å)		a(Å)		a(Å)
CaF_2	5.4626	PbO_2	5.349	Li_2O	4.6114	K_2O	6.449
SrF_2	5.800	CeO_2	5.4110	Li_2S	5.710	K_2S	7.406
$SrCl_2$	6.9767	PrO_2	5.392	Li_2Se	6.002	K_2Se	7.692
BaF_2	6.2001	ThO_2	5.600	Li_2Te	6.517	K_2Te	8.168
$BaCl_2$	7.311	PaO_2		Na_2O	5.55	Rb_2O	6.74
CdF_2	5.3895	UO_2	5.372	Na_2S	6.539	Rb_2S	7.65
HgF_2	5.5373	NpO_2	5.4334	Na_2Se	6.823		
EuF_2	5.836	PuO_2	5.386	Na_2Te	7.329		
β-PbF_2	5.940	AmO_2	5.376				
		CmO_2	5.3598				

$\gamma = 90°$), and involves simple trigonometric calculations. For example, in the rock salt structure, the anion–cation distance is $a/2$ and the anion–anion distance is $a/\sqrt{2}$. As an aid to rapid calculation of interatomic distances, formulae are given in Table 7.8 for the more important structure types. These may be used in conjunction with the tables of unit cell dimensions (Table 7.5, etc.) to make calculations on specific compounds.

Table 7.8 *Calculation of interatomic distances in some simple structures*

Structure type	Distance	Number of such distances	Magnitude of separation in terms of unit cell dimensions
Rock salt (cubic)	Na–Cl	6	$a/2 = 0.5a$
	Cl–Cl	12	$a/\sqrt{2} = 0.707a$
	Na–Na	12	$a/\sqrt{2} = 0.707a$
Zinc blende (cubic)	Zn–S	4	$a\frac{\sqrt{3}}{4} = 0.433a$
	Zn–Zn	12	$a/\sqrt{2} = 0.707a$
	S–S	12	$a/\sqrt{2} = 0.707a$
Fluorite (cubic)	Ca–F	4 or 8	$a\frac{\sqrt{3}}{4} = 0.433a$
	Ca–Ca	12	$a/\sqrt{2} = 0.707a$
	F–F	6	$a/2 = 0.5a$
Wurtzite* (hexagonal)	Zn–S	4	$a\sqrt{\frac{3}{8}} = 0.612a = \frac{3c}{8} = 0.375c$
	Zn–Zn	12	$a = 0.612c$
	S–S	12	$a = 0.612c$
Nickel arsenide* (hexagonal)	Ni–As	6	$a/\sqrt{2} = 0.707a = 0.433c$
	As–As	12	$a = 0.612c$
	Ni–Ni	2	$c/2 = 0.5c = 0.816a$
	Ni–Ni	6	$a = 0.612c$
Cesium chloride (cubic)	Cs–Cl	8	$a\frac{\sqrt{3}}{2} = 0.866a$
	Cs–Cs	6	a
	Cl–Cl	6	a
Cadmium iodide (hexagonal)	Cd–I	6	$a/\sqrt{2} = 0.707a = 0.433c$
	I–I	12	$a = 0.612c$
	Cd–Cd	6	$a = 0.612c$

*These formulae do not necessarily apply when c/a is different from the ideal value of 1.633.

Consideration of the anion and cation arrangements in the three structure types described above shows that the concept of c.p. anions with cations in interstitial sites begins to break down in the fluorite structure. Thus, while the antifluorite structure of, for example, Na_2O may be regarded as containing cubic close packed O^{2-} ions with Na^+ ions in tetrahedral sites, in the fluorite structure of, for example, CaF_2, it is necessary to regard the Ca^{2+} ions as forming the c.c.p. array with the F^- ions occupying tetrahedral interstitial sites. In CaF_2, although the Ca^{2+} ions have the same arrangement as in a c.c.p. arrangement of spheres, the Ca^{2+} ions are well separated from each other; from Tables 7.7 and 7.8, Ca–Ca = 3.86 Å, which is much larger than the diameter of a Ca^{2+} ion (depending on which table of ionic radii is consulted, the diameter of a Ca^{2+} ion is in the range ~ 2.2 to 2.6 Å). Therefore, CaF_2 is a good example of a eutactic structure.

The fluorine–fluorine distance in CaF_2 is 2.73 Å, which indicates that the fluorines are approximately contacting ($r_{F^-} = 1.2$ to 1.4 Å). Although the primitive cubic array of F^- ions in CaF_2 is not a c.p. arrangement, the anions are approximately in contact and this is perhaps a more realistic way of describing the structure than as containing a c.c.p. array of Ca^{2+} ions.

7.2.2 Wurtzite (ZnS) and nickel arsenide (NiAs)

These structures have in common a hexagonal close packed arrangement of anions and differ only in the positions of the cations, as follows:

Wurtzite: T_+(or T_-) sites occupied; T_-(or T_+), O empty

Nickel arsenide: O sites occupied; T_+, T_- empty.

These structures are the hexagonal close packed analogues of the cubic close packed, sphalerite and rock salt structures. Note that there is no hexagonal equivalent of the fluorite and antifluorite structures.

Both wurtzite and nickel arsenide have hexagonal symmetry and unit cells. A unit cell containing hexagonal close packed anions is shown in Fig. 7.19(a). It is less easy to visualize and draw on paper than a cubic cell because of the γ angle of 120°. The unit cell contains two anions, one at the origin and one inside the cell. Their coordinates are:

$$0, 0, 0; \qquad \tfrac{1}{3}, \tfrac{2}{3}, \tfrac{1}{2}$$

In Fig. 7.19(b) is shown a projection down c of the same structure. Close packed layers occur in the basal plane, i.e. at $c = 0$ (open circles) and at $c = \frac{1}{2}$ (shaded circles). The layer arrangement at $c = 0$ is repeated at $c = 1$ and therefore the stacking sequence is hexagonal ...ABABA.... Atoms 1 to 4 in the basal plane outline the base of the unit cell (dashed).

The contents of one unit cell are shown in Fig. 7.19(c). Dashed circles represent atoms at the top four corners of the unit cell, i.e. at $c = 1$.

In metals which have hexagonal close packed structures, metal atoms are in contact, e.g. 1 and 2, 1 and 4, 1 and 5. In eutactic close packed ionic structures, however, the anions may be pushed apart by the cations in the interstitial sites

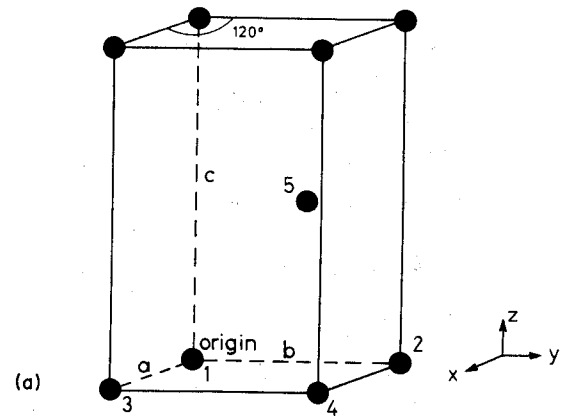

(a)

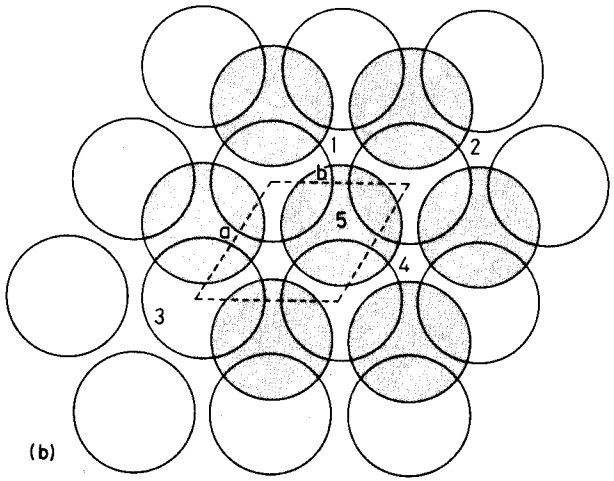

(b)

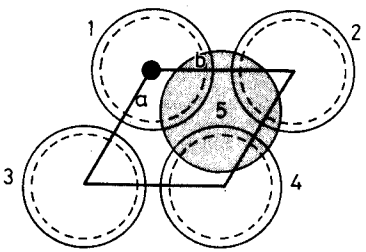

(c)

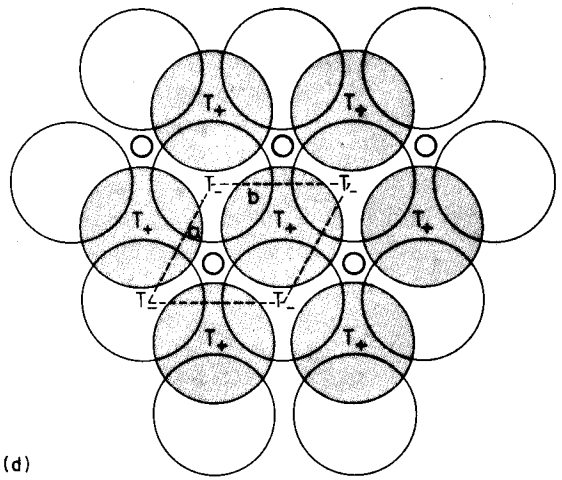

(d)

T_-	:	$0, 0, {}^{3}/_{8}$	;	${}^{1}/_{3}, {}^{2}/_{3}, {}^{7}/_{8}$
T_+	:	${}^{1}/_{3}, {}^{2}/_{3}, {}^{1}/_{8}$	;	$0, 0, {}^{5}/_{8}$
0	:	${}^{2}/_{3}, {}^{1}/_{3}, {}^{1}/_{4}$	;	${}^{2}/_{3}, {}^{1}/_{3}, {}^{3}/_{4}$
ANION	:	$0, 0, 0$		${}^{1}/_{3}, {}^{2}/_{3}, {}^{1}/_{2}$

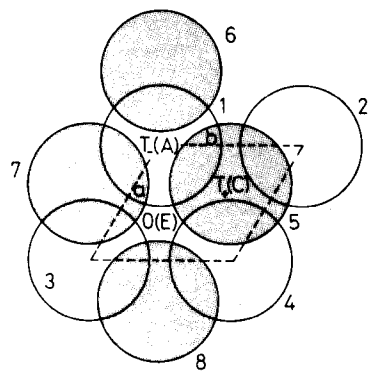

(e)

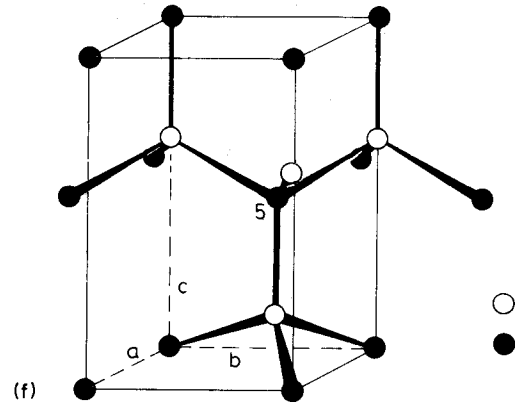

(f)

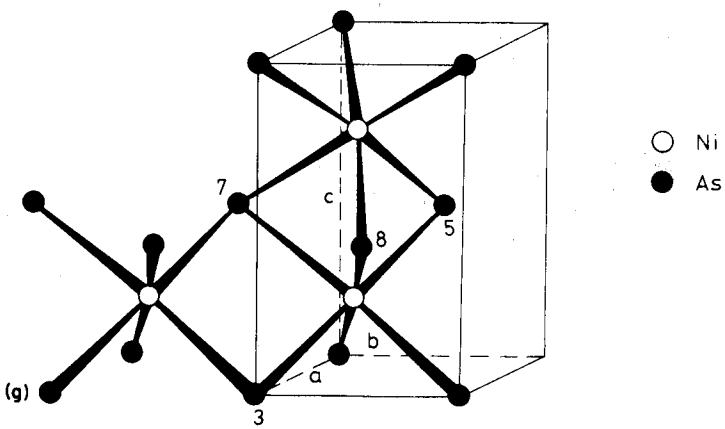

(g)

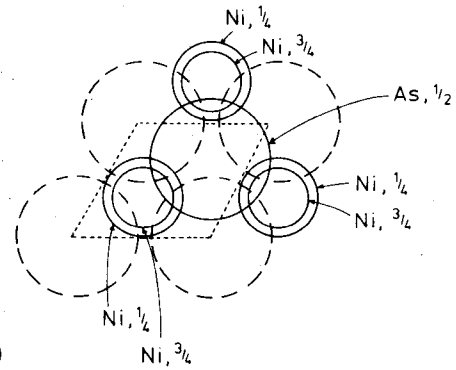

(h)

the tetrahedron, i.e. at one quarter of the vertical distance from base to apex (Appendix 1). Since the apex and base are at $c = 0$ and $c = \frac{1}{2}$, this T_- site is at $c = \frac{3}{8}$. In practice the occupant of this T_- site in the wurtzite structure may not be at exactly 0.375*c*. For those structures which have been studied accurately (Table 7.9), values range from 0.345 to 0.385; the letter *u* is used to represent the fractional *c* value.

The three anions (5 to 7) at $c = \frac{1}{2}$ that form the base of this T_- site, A, also form the base of a T_+ site, B (not shown), centred at 0, 0, $\frac{5}{8}$. The apex of the latter tetrahedron is the anion at the top corner with coordinates 0, 0, 1. Another T_+ site, C, is shown in Fig. 7.19(e) at $\frac{1}{3}, \frac{2}{3}, \frac{1}{8}$. It is coordinated to anions 1, 2 and 4 in the basal plane at three corners of the unit cell and to anion 5 at $\frac{1}{3}, \frac{2}{3}, \frac{1}{2}$. The triangular base of this site, at $c = 0$, is shared with a T_- site underneath (not shown) at $\frac{1}{3}, \frac{2}{3}, -\frac{1}{8}$. The equivalent T_- site that lies inside the unit cell, D (not shown) is at $\frac{1}{3}, \frac{2}{3}, \frac{7}{8}$.

Octahedral site E, in Fig. 7.19(e) is coordinated to anions 1, 3 and 4 at $c = 0$ and to anions 5, 7 and 8 at $c = \frac{1}{2}$. The centre of gravity of the octahedron lies midway between these two groups of anions and has coordinates $\frac{2}{3}, \frac{1}{3}, \frac{1}{4}$. The second octahedral site, F (not shown) in the cell lies above E at $c = \frac{3}{4}$ and has coordinates $\frac{2}{3}, \frac{1}{3}, \frac{3}{4}$. The three anions 5, 7 and 8 are therefore common to the two octahedra.

The coordination environments of the cations in wurtzite and NiAs are emphasized in Fig. 7.19(f) and (g). Zinc is shown in T_+ sites and forms ZnS_4 tetrahedra, (f), which link up at their corners to form a three-dimensional network, as in (j). A similar structure results on considering the tetrahedra formed by four zinc atoms around a sulphur and the manner in which these SZn_4 tetrahedra are linked. The tetrahedral environment of the sulphur ion (5) is shown in (f). The SZn_4 tetrahedron which it forms points downwards, in contrast to the ZnS_4 tetrahedra which all point upwards; on turning the SZn_4 tetrahedra upside down, however, the same structure results.

Comparing larger scale models of the zinc blende (Fig. 7.17b) and wurtzite (Fig. 7.19j) structures, they are clearly very similar and can both be regarded as networks of tetrahedra. In zinc blende, layers of tetrahedra form an ABC stacking sequence and the orientation of the tetrahedra within each layer is identical. In wurtzite, however, the layers form an AB sequence and alternate layers are rotated by 180° about *c* relative to each other.

The $NiAs_6$ octahedra in NiAs are shown in Fig. 7.19(g). They share one pair of opposite faces (e.g. the face formed by arsenic ions 5, 7 and 8) to form chains of face-sharing octahedra that run parallel to *c*. In the *ab* plane, however, the octahedra share only common edges: arsenic ions 3 and 7 are shared between two octahedra such that chains of edge-sharing octahedra form parallel to *c*. Similarly, chains of edge-sharing octahedra form parallel to *a* (not shown), a more extended view of the octahedra and their linkages is shown in Fig. 7.19(k).

The NiAs structure is unusual in that the anions and cations have the same coordination number but do not have the same coordination environment. In the other AB structures—rock salt, sphalerite, wurtzite and CsCl—anions and cations are interchangeable and have the same coordination number and environment. Since the cation : anion ratio is 1:1 in NiAs and the nickel

coordination is octahedral, the arsenic ions must also be six coordinate. However, the six nickel neighbours are arranged as in a trigonal prism and not octahedrally. This is shown for arsenic at $c = \frac{1}{2}$ in Fig. 7.19(h), which is coordinated to three nickel ions at $c = \frac{1}{4}$ and to three at $c = \frac{3}{4}$. The two sets of nickel ions are superposed in projection down *c* and give the trigonal prismatic coordination for arsenic. (Note that in a similar projection for octahedral coordination, the two sets of three outer atoms appear to be staggered relative to each other, as in Fig. 7.19(e) for octahedral site E.)

The NiAs structure may also be regarded as built of $AsNi_6$ trigonal prisms, therefore, which link up by sharing edges to form a three-dimensional array. In Fig. 7.19(i) each triangle represents a prism in projection down *c*. The prism edges that run parallel to *c*, i.e. those formed by nickel ions at $c = \frac{1}{4}$ and $\frac{3}{4}$ in Fig. 7.19(h), are shared between three prisms. Thus the vertical edge at y (in projection it is a point) is shared between three prisms and therefore three arsenic ions at $c = \frac{1}{2}$. Prism edges that lie in the *ab* plane are shared between only two prisms, however. In Fig. 7.19(i), the edge xy is shared between arsenic ions at $c = \frac{1}{2}$ and $c = 0$.

The structure may be regarded as built up of layers of prisms; two layers are shown in Fig. 7.19(i) centred at $c = \frac{1}{2}$ and $c = 0$ and are rotated by 180° about *c* relative to each other. The next layer of prisms, at $c = 1$, is in the same orientation as the layer at $c = 0$ and hence, an ...ABABA... hexagonal stacking sequence arises. This is shown further in Fig. 7.19(l).

A selection of compounds which have wurtzite and NiAs structures is given in Tables 7.9 and 10 with values of their hexagonal cell parameters *a* and *c*. The wurtzite structure is formed mainly by chalcogenides of some divalent metals and may be regarded as a fairly ionic structure (Chapter 8). The NiAs structure is a more metallic structure and is adopted by a variety of intermetallic compounds and by some transition metal chalcogenides (S, Se, Te). The value of the ratio *c*/*a*

Table 7.10 *Some compounds with the NiAs structure.* (Data taken from Wyckoff, 1971, Vol. 1)

	a(Å)	*c*(Å)	*c*/*a*		*a*(Å)	*c*(Å)	*c*/*a*
NiS	3.4392	5.3484	1.555	CoS	3.367	5.160	1.533
NiAs	3.602	5.009	1.391	CoSe	3.6294	5.3006	1.460
NiSb	3.94	5.14	1.305	CoTe	3.886	5.360	1.379
NiSe	3.6613	5.3562	1.463	CoSb	3.866	5.188	1.342
NiSn	4.048	5.123	1.266	CrSe	3.684	6.019	1.634
NiTe	3.957	5.354	1.353	CrTe	3.981	6.211	1.560
FeS	3.438	5.880	1.710	CrSb	4.108	5.440	1.324
FeSe	3.637	5.958	1.638	MnTe	4.1429	6.7031	1.618
FeTe	3.800	5.651	1.487	MnAs	3.710	5.691	1.534
FeSb	4.06	5.13	1.264	MnSb	4.120	5.784	1.404
δ′-NbN*	2.968	5.549	1.870	MnBi	4.30	6.12	1.423
PtB*	3.358	4.058	1.208	PtSb	4.130	5.472	1.325
PtSn	4.103	5.428	1.323	PtBi	4.315	5.490	1.272

* Anti-NiAs structure.

is approximately constant in the family of wurtzite structures but varies considerably between the different compounds with the NiAs structure. This is associated with the presence of metallic bonding which arises from metal–metal interactions in the c direction, as follows:

Let us consider the environment of nickel and arsenic ions.
Each arsenic is surrounded by (Table 7.8):
6 nickel ions (in a trigonal prism) at distance $0.707a$
12 arsenic ions (h.c.p. arrangement) at distance a
Each nickel is surrounded by:
6 arsenic ions (octahedrally) at distance $0.707a$
2 nickel ions (linearly, parallel to c) at distance $0.816a$ (i.e. $c/2$)
6 nickel ions (hexagonally, in ab plane) at distance a

The main effect of changing the value of the c/a ratio is to alter the nickel–nickel distance parallel to c. Thus, in FeTe, $c/a = 1.49$, and hence the iron–iron distance parallel to c is reduced to $0.745a$ (i.e. $c/2 = \frac{1}{2}(1.49a)$), thereby bringing these iron ions into closer contact and increasing the metallic bonding in the c direction. Quantitative calculations of the effect of changing the c/a ratio are more difficult to make since it is not readily possible to distinguish between, for example, an increase in a and a decrease in c, either of which could cause the same effect on the c/a ratio.

The non-occurrence of AX_2 compounds whose structures are the hexagonal equivalent of the cubic fluorite and antifluorite structures has already been mentioned. This may be understood by considering the various interatomic distances that would be present in such a structure. A hexagonal fluorite-like structure, AX_2, would have hexagonal packed A cations with X anions fully occupying T_+ and T_- sites. From Fig. 7.19(d), X ions would occupy, for example, sites at 0, 0, $\frac{3}{8}$(T_-) and 0, 0, $\frac{5}{8}$(T_+), thereby giving an X–X distance of $c/4 = 0.25c$. This compares with the A–X distance (as in wurtzite, Table 7.8) of $0.375c$. Since the shortest interatomic separations in ionic structures are almost always cation–anion contacts, it is most unlikely that a structure would exist in which anion–anion distances were much shorter than anion–cation distances (and vice versa for the equivalent antifluorite structure).

7.2.3 Caesium chloride, CsCl

The unit cell of CsCl is shown in Fig. 7.20. It is primitive cubic, containing Cl^- ions at the corners and a Cs^+ ion at the body centre, or vice versa (note that it is *not* body centred cubic since there are different ions at corner and body centre positions). The coordination numbers of both Cs^+ and Cl^- are eight with interatomic distances of $0.866a$ (Table 7.8). The CsCl structure cannot be regarded as close packed. In a c.p. structure, e.g. NaCl, each Cl^- has twelve other Cl^- ions as next nearest neighbours, which is a characteristic feature of c.p. (or eutactic c.p.) structures. In CsCl, however, each Cl has only six Cl^- ions as next nearest neighbours (arranged octahedrally). Some compounds which exhibit the

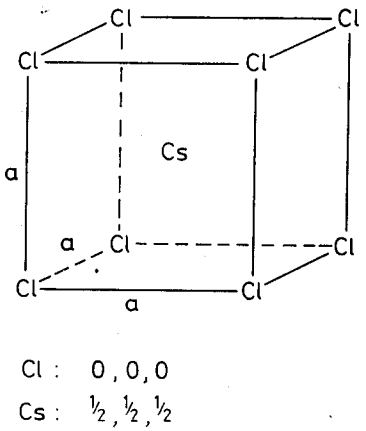

Fig. 7.20 The primitive cubic unit cell of CsCl

Table 7.11 *Some compounds with the CsCl structure*

	a(Å)		a(Å)
CsCl	4.123	CuZn	2.945
CsBr	4.286	CuPd	2.988
CsI	4.5667	AuMg	3.259
CsCN	4.25	AuZn	3.19
NH_4Cl	3.8756	AgZn	3.156
NH_4Br	4.0594	LiAg	3.168
TlCl	3.8340	AlNi	2.881
TlBr	3.97	LiHg	3.287
TlI	4.198	MgSr	3.900

CsCl structure are given in Table 7.11. They fall into two groups, halides of large monovalent elements and a variety of intermetallic compounds.

7.2.4 Other AX structures

There are five main AX structure types: rock salt, CsCl, NiAs, sphalerite and wurtzite, each of which is found in a large number of compounds. There is also a considerable number of less common AX structures. Some may be regarded as distorted variants of one of the main structure types, e.g.:

(a) FeO at low temperatures, < 90 K, has a rock salt structure which has undergone a slight rhombohedral distortion (the α angle is increased from 90 to 90.07° by a slight compression along one threefold axis). This rhombohedral distortion is associated with magnetic ordering in FeO at low temperatures, Chapter 16.

(b) TlF has a rock salt related structure in which the f.c.c. cell is distorted into a face centred orthorhombic cell by changing the lengths of all three cell axes by different amounts.

(c) NH_4CN has a distorted CsCl structure (as in NH_4Cl) in which the CN^- ions do not assume spherical symmetry but are oriented parallel to [110] directions (i.e. face diagonals). This distorts the symmetry to tetragonal and effectively increases *a* relative to *c*.

Other AX compounds have completely different structures, e.g.:

(a) Compounds of the d^8 ions, Pd and Pt (in PdO, PtS, etc.) often have a square planar coordination for the cation with tetragonal or orthorhombic symmetry for the structure as a whole; d^9 ions show this effect as well, e.g. Cu in CuO.

(b) Compounds of heavy *p*-block ions in their lower oxidation states (Pb^{2+}, Bi^{3+}, etc.) often have distorted polyhedra in which the cation exhibits the *inert pair effect*. Thus PbO and SnO have structures in which the M^{2+} ion has four O^{2-} neighbours to one side giving a square pyramidal arrangement; the O^{2-} coordination is a more regular tetrahedron of M^{2+} ions. InBi has a similar structure in which Bi^{3+} is the ion with the inert pair effect and the irregular coordination.

7.2.5 Rutile (TiO_2), CdI_2, $CdCl_2$ and Cs_2O structures

The title structures together with the fluorite structure (Section 7.2.2) constitute the main AX_2 structure types. Rutile, TiO_2, has been described in some detail in Chapter 6; it may be regarded as having a distorted hexagonal close packed oxide array or, alternately, as a tetragonal packed oxide array. In either description, one half of the octahedral sites are occupied by Ti^{4+}. The TiO_6 octahedra thus formed link up by sharing one pair of opposite edges with neighbouring octahedra to form infinite chains parallel to *c*. These chains link at their corners with neighbouring chains to form a three-dimensional network of octahedra.

The octahedral sites in an ideal h.c.p. anion array are shown in Fig. 7.21(a). While all these sites are occupied in NiAs (Fig. 7.19h), only half are occupied in rutile and in such a manner that alternate rows of octahedral sites are full and empty. It should be emphasized again that this is an idealized situation since, in rutile, the oxide layers (parallel to the plane of the paper in Fig. 7.21a) are not planar but are buckled. The orientation of the tetragonal unit cell in rutile is shown in Fig. 7.21(a).

Parallel to the tetragonal *c* axis, the TiO_6 octahedra share edges. This is shown in Fig. 7.21(b) for two octahedra with oxygens 1 and 2 forming the common edge and in Appendix 2 for several octahedra similarly linked to form a chain.

Two main groups of compounds exhibit the rutile structure (Table 7.12): oxides of some tetravalent metal ions and fluorides of small divalent metal ions.

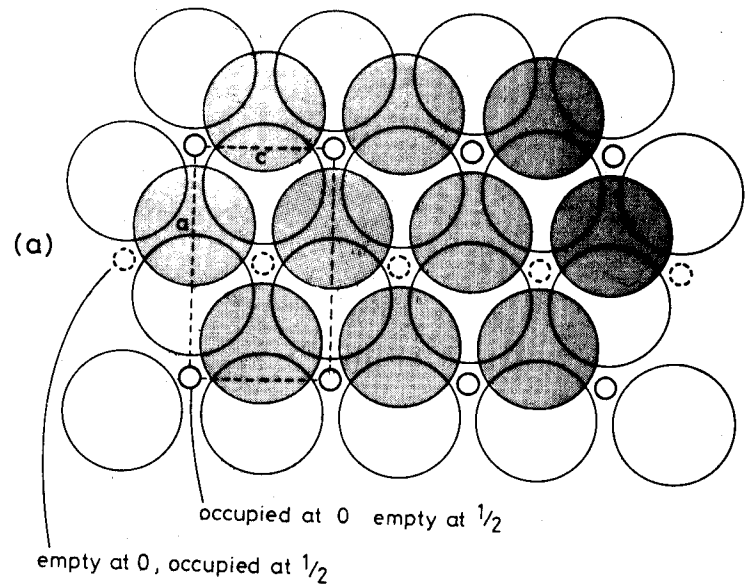

Fig. 7.21 The rutile structure: (a) in idealized form, with planar oxide layers; (b) edge-sharing octahedra

In both cases, these M^{4+} and M^{2+} ions are too small to form the fluorite structure with O^{2-} and F^-, respectively. The rutile structure may be regarded as an essentially ionic structure.

The CdI_2 structure is nominally very similar to rutile because it also may be described as a hexagonal close packed anion array in which half the octahedral sites are occupied by M^{2+} ions. The manner of occupancy of the octahedral sites is quite different, however, since in CdI_2, entire layers of octahedral sites are occupied and these alternate with layers of empty sites (Fig. 7.22). CdI_2 is therefore a layered material in both its crystal structure and properties, in contrast to rutile which has a more rigid, three-dimensional character.

Two iodide layers in a hexagonal close packed array are shown in Fig. 7.22(a) with the octahedral sites in between occupied by Cd^{2+}. To either side of the

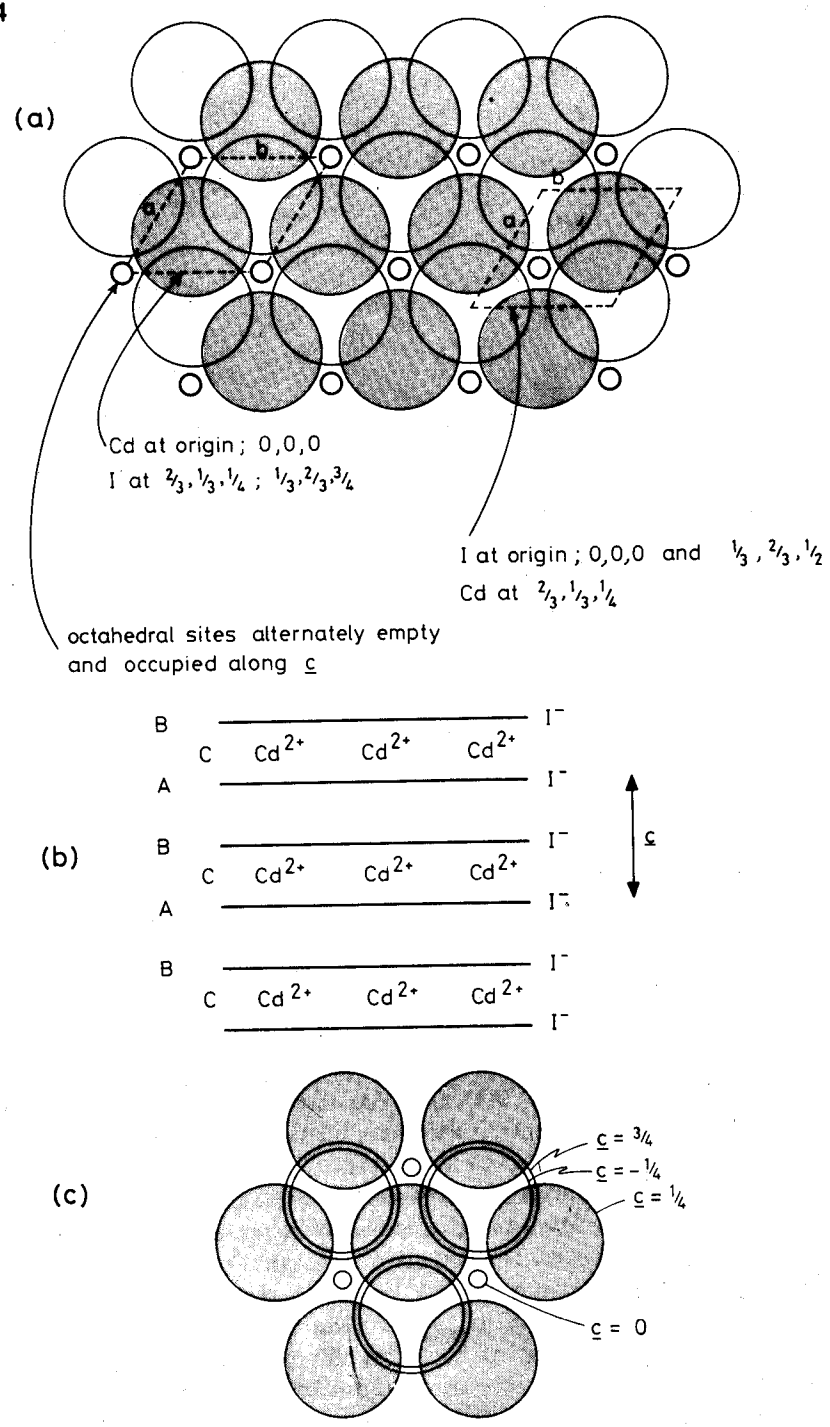

Fig. 7.22 The CdI_2 structure: (a) the unit cell, with two possible choices of origin, (b) the layer stacking sequence, (c) the coordination environment of I

Table 7.12 *Some compounds with the rutile structure.* (Data taken from Wyckoff, 1971, Vol. 1)

	a(Å)	c(Å)	x		a(Å)	c(Å)	x
TiO_2	4.5937	2.9581	0.305	CoF_2	4.6951	3.1796	0.306
CrO_2	4.41	2.91		FeF_2	4.6966	3.3091	0.300
GeO_2	4.395	2.859	0.307	MgF_2	4.623	3.052	0.303
IrO_2	4.49	3.14		MnF_2	4.8734	3.3099	0.305
β-MnO_2	4.396	2.871	0.302	NiF_2	4.6506	3.0836	0.302
MoO_2	4.86	2.79		PdF_2	4.931	3.367	
NbO_2	4.77	2.96		ZnF_2	4.7034	3.1335	0.303
OsO_2	4.51	3.19					
PbO_2	4.946	3.379					
RuO_2	4.51	3.11					
SnO_2	4.7373	3.1864	0.307				
TaO_2	4.709	3.065					
WO_2	4.86	2.77					

iodide layers, the octahedral sites are empty. Compare this with NiAs (Fig. 7.19d and h) which has the same anion arrangement but with all the octahedral sites occupied. The layer stacking sequence along c in CdI_2 is shown schematically in Fig. 7.22(b) and emphasizes the layered nature of the CdI_2 structure. I^- layers form an ...ABABA... stacking sequence. Cd^{2+} ions occupy octahedral sites which may be regarded as the C positions relative to the AB positions for I^-. The CdI_2 structure may be regarded as a sandwich structure in which Cd^{2+} ions are sandwiched between layers of I^- ions and adjacent sandwiches are held together by weak van der Waals bonds between the layers of I^- ions. In this sense, CdI_2 has certain similarities to molecular structures. For example, solid CCl_4 has strong C—Cl bonds within the molecule but only weak Cl—Cl bonds between adjacent molecules. Because the intermolecular forces are weak, CCl_4 is volatile with a low melting and boiling point. In the same way, CdI_2 may be regarded as an infinite sandwich 'molecule' in which there are strong Cd—I bonds within the molecule but weak van der Waals bonds between adjacent molecules.

The coordination of the I^- ion in CdI_2 is shown in Fig. 7.22(c). An I^- ion at $c = \frac{1}{4}$ (shaded) has three close Cd^{2+} neighbours to one side at $c = 0$. The next nearest neighbours are the twelve I^- ions that form the h.c.p. array.

The layered nature of CdI_2 is emphasized further by constructing a model from polyhedra: CdI_6 octahedra link up at their edges to form infinite sheets (Appendix 2), but there are no direct polyhedral linkages between adjacent sheets. A self-supporting, three-dimensional model of octahedra cannot be made for CdI_2, therefore, unlike, for example, rutile.

Some compounds which have the CdI_2 structure are listed in Table 7.13. This structure occurs mainly in transition metal iodides and also with some bromides, chlorides and hydroxides.

The cadmium chloride structure is closely related to that of CdI_2 and differs only in the nature of the anion packing: Cl^- ions are cubic close packed in $CdCl_2$

Table 7.13 *Some compounds with the CdI_2 structure.* (Data taken from Wyckoff, 1971, Vol. 1)

	a(Å)	c(Å)		a(Å)	c(Å)
CdI_2	4.24	6.84	VBr_2	3.768	6.180
CaI_2	4.48	6.96	$TiBr_2$	3.629	6.492
CoI_2	3.96	6.65	$MnBr_2$	3.82	6.19
FeI_2	4.04	6.75	$FeBr_2$	3.74	6.17
MgI_2	4.14	6.88	$CoBr_2$	3.68	6.12
MnI_2	4.16	6.82	$TiCl_2$	3.561	5.875
PbI_2	4.555	6.977	VCl_2	3.601	5.835
ThI_2	4.13	7.02	$Mg(OH)_2$	3.147	4.769
TiI_2	4.110	6.820	$Ca(OH)_2$	3.584	4.896
TmI_2	4.520	6.967	$Fe(OH)_2$	3.258	4.605
VI_2	4.000	6.670	$Co(OH)_2$	3.173	4.640
YbI_2	4.503	6.972	$Ni(OH)_2$	3.117	4.595
ZnI_2(I)	4.25	6.54	$Cd(OH)_2$	3.48	4.67

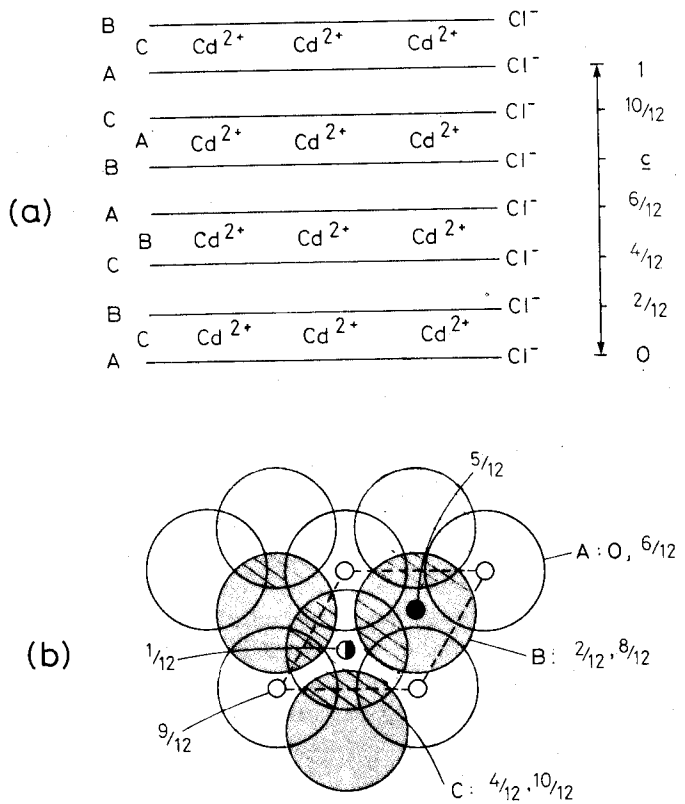

Fig. 7.23 The $CdCl_2$ structure

whereas I^- ions are hexagonal close packed in CdI_2. $CdCl_2$ and CdI_2 form a pair of closely related structures, therefore, in the same way that wurtzite and zinc blende or rock salt and nickel arsenide differ only in the anion stacking sequence.

The $CdCl_2$ structure may be represented by a hexagonal unit cell, although a smaller rhombohedral cell can also be chosen. The base of the hexagonal cell is of similar size and shape to that in CdI_2 but the c axis of $CdCl_2$ is three times as long as c in CdI_2. This is because in $CdCl_2$, the Cd^{2+} positions, and the $CdCl_6$ octahedra, are staggered along c and give rise to a three-layer repeat for Cd^{2+} ions (CBA) and a six-layer repeat for Cl^- ions (ABCABC) (Fig. 7.23). In contrast, in CdI_2, the Cd^{2+} positions and the CdI_6 octahedra are stacked on top of each other and the c repeat contains only two I^- layers (AB) and one Cd^{2+} layer (C).

The unit cell of $CdCl_2$ in projection down c is shown in Fig. 7.23(b). Chloride layers occur at $c = 0$(A), $\frac{2}{12}$(B) and $\frac{4}{12}$(C) and this sequence is repeated at $c = \frac{6}{12}$, $\frac{8}{12}$ and $\frac{10}{12}$. Between those Cl^- layers at 0 and $\frac{2}{12}$ are Cd^{2+} ions in the octahedral sites at $\frac{1}{12}$. However, the octahedral sites between Cl^- layers at $\frac{2}{12}$ and $\frac{4}{12}$ are empty (these sites, at $c = \frac{3}{12}$, are directly below the Cd^{2+} ions at $\frac{9}{12}$).

The $CdCl_2$ structure is a layered structure, similar to CdI_2, and many of the comments made about structure and bonding in CdI_2 apply equally well to $CdCl_2$. Some compounds which have the $CdCl_2$ structure are given in Table 7.14. It also occurs with a variety of transition metal halides.

The structure of Cs_2O is unusual since it may be regarded as an anti-$CdCl_2$ structure (as in fluorite and antifluorite structures). Cs^+ ions form cubic close packed layers and oxide ions occupy the octahedral sites between alternate pairs of caesium layers. This raises some interesting questions because caesium is the most electropositive element and caesium salts are usually regarded as highly ionic. However, the structure of Cs_2O clearly shows that Cs^+ ions are not surrounded by anions, as expected for an ionic structure, but have only three oxide neighbours, all located at one side. The structure is held together, in three dimensions, by bonding between caesium ions in adjacent layers.

It may be that the structure of Cs_2O does not reflect any peculiar type of bonding but rather that it is the only structural arrangement which is feasible for a compound of this formula and for ions of this size. Thus, from the formula, the

Table 7.14 *Some compounds with the $CdCl_2$ structure.* (Data taken from Wyckoff, 1971, Vol. 1)

	a(Å)	c(Å)		a(Å)	c(Å)
$CdCl_2$	3.854	17.457	$NiCl_2$	3.543	17.335
$CdBr_2$	3.95	18.67	$NiBr_2$	3.708	18.300
$CoCl_2$	3.544	17.430	NiI_2	3.892	19.634
$FeCl_2$	3.579	17.536	$ZnBr_2$	3.92	18.73
$MgCl_2$	3.596	17.589	ZnI_2	4.25	21.5
$MnCl_2$	3.686	17.470	Cs_2O*	4.256	18.99

*Cs_2O has an anti-$CdCl_2$ structure.

coordination numbers of Cs^+ and O^{2-} must be in the ratio of 1:2; since Cs^+ is considerably larger than O^{2-}, the maximum possible coordination number of oxygen by caesium may be six, which then leads to a coordination number of three for Cs^+.

A related question arises with the structures of the other alkali oxides, in particular K_2O and Rb_2O. These have the antifluorite structure with coordination numbers of four and eight for M^+ and O^{2-}, respectively. These compounds are unusual since Rb^+ is normally far too large a cation to enter into tetrahedral coordination with oxygen. However, if there is no feasible alternative structure, then perhaps Rb^+ ions have no choice but to enter the tetrahedral sites. With Cs_2O, tetrahedral coordination of Cs^+ by O^{2-} is probably impossible and hence it adopts the anti-$CdCl_2$ structure rather than the antifluorite structure. Thermodynamic data support these observations since neither Cs_2O nor Rb_2O are very stable: they oxidize readily to give peroxides, M_2O_2, and superoxides, MO_2, which contain much larger anions.

7.3 Silicate structures—some tips to understanding them

Silicates, especially many minerals, often have very complicated formulae. The purpose of this section is not to give a review of the crystal structures of silicates but simply to show that a considerable amount of structural information may be obtained from their chemical formulae. Using certain guidelines one can appreciate, without the necessity of remembering a large number of complex formulae, whether a particular silicate is a three-dimensional framework structure, whether it is sheet-like or chain-like, etc.

It is common practice to regard many silicate structures as composed of cations and silicate anions. Various types of silicate anion are possible, ranging from the extremes of isolated SiO_4^{4-} tetrahedra in orthosilicates such as olivine (Mg_2SiO_4), to infinite three-dimensional frameworks, as in silica itself (SiO_2). The structures of the various silicate anions are based on certain principles:

(1) Almost all silicate structures are built of SiO_4 tetrahedra.
(2) The SiO_4 tetrahedra may link up by sharing corners to form larger polymeric units.
(3) No more than two SiO_4 tetrahedra may share a common corner (i.e. oxygen).
(4) SiO_4 tetrahedra never share edges or faces with each other.

Exceptions to (1) are structures in which silicon is octahedrally coordinated to oxygen as in, for instance, one of the polymorphs of SiP_2O_7. The number of these exceptions is very small, however, and we can regard SiO_4 tetrahedra as the normal building block in silicate structures. Guidelines (3) and (4) are concerned respectively with maintaining local electroneutrality and with ensuring that highly charged cations, such as Si^{4+}, are not too close together. They are discussed in more detail in Chapter 8.

Let us see now how the structures of silicate anions are related, in a simple way to their formulae. The important factor in relating formula to structure type is the silicon to oxygen ratio. This ratio is variable since two types of oxygen may be

Table 7.15 *Relation between chemical formula and silicate anion structure.*

Si:O ratio‡	Number of oxygens per Si: bridging	non-bridging	Type of silicate anion	Examples
1:4	0	4	isolated SiO_4^{4-}	Mg_2SiO_4 olivine, Li_4SiO_4
1:3.5	1	3	dimer $Si_2O_7^{6-}$	$Ca_3Si_2O_7$ rankinite, $Sc_2Si_2O_7$ thortveite
1:3	2	2	chains $(SiO_3)_n^{2n-}$	Na_2SiO_3, $MgSiO_3$ pyroxene
			rings, eg $Si_3O_9^{6-}$	$CaSiO_3$*, $BaTiSi_3O_9$ benitoite
			$Si_6O_{18}^{12-}$	$Be_3Al_2Si_6O_{18}$ beryl
1:2.5	3	1	infinite sheets $(Si_2O_5)_n^{2n-}$	$Na_2Si_2O_5$
1:2	4	0	3D framework	SiO_2†

* $CaSiO_3$ is dimorphic. One polymorph has $Si_3O_9^{6-}$ rings. The other polymorph has infinite $(SiO_3)_n^{2n-}$ chains.
† The three main polymorphs of silica, quartz, tridymite and cristobalite each have a different kind of 3D framework structure.
‡ In some structures, as in sphene, $CaTiSiO_5$ and Ca_3SiO_5, the Si:O ratio is less than 1:4; these contain SiO_4^{4-} tetrahedra together with extra oxygens entirely unconnected to any silicon.

distinguished in the silicate anions: *bridging oxygens* and *non-bridging oxygens*. Bridging oxygens are those that link up, or are common to, two tetrahedra. Effectively, they may be regarded as belonging half to one Si and half to another Si. In evaluating the net Si:O ratio, bridging oxygens count as $\frac{1}{2}$. Non-bridging oxygens are those that are linked to only one silicon or silicate tetrahedron. They may also be called terminal oxygens. In order to maintain charge balance, non-bridging oxygens must also be linked to other cations in the crystal structure. In evaluating the overall Si:O ratio, non-bridging oxygens count as 1.

The overall Si:O ratio in a silicate crystal structure depends on the relative number of bridging and non-bridging oxygens. Some examples are given in Table 7.15. In these, the alkali and alkaline earth cations do not form part of the silicate anion whereas in certain other cases, e.g. in aluminosilicates, cations such as Al^{3+} may substitute for silicon in the silicate anion. The examples given in the Table are all straightforward and one may deduce the type of silicate anion directly from the chemical formula.

Many other more complex examples could be given. In these, although the detailed structure cannot be deduced from the formula, one can at least get an approximate idea of the type of silicate anion. For example, in the phase $Na_2Si_3O_7$, the Si:O ratio is 1:2.33. This corresponds to a structure in which, on average, two thirds of an oxygen per SiO_4 tetrahedron are non-bridging. Clearly, therefore, some of the SiO_4 tetrahedra in this structure must be composed entirely

of bridging oxygens whereas others contain one non-bridging oxygen. The structure of the silicate anion would therefore be expected to be something between an infinite sheet and a 3D framework. In fact, the structure contains an infinite, double-sheet silicate anion in which two thirds of the silicate tetrahedra have one non-bridging oxygen.

The relation between formula and anion structure becomes more complex in cases where ions such as Al^{3+} may substitute for Si^{4+} in the silicate anion. Examples are as follows.

The plagioclase feldspars are a family of aluminosilicates typified by albite, $NaAlSi_3O_8$ and anorthite, $CaAl_2Si_2O_8$. In both of these Al is partly replacing Si in the silicate anion. It is therefore appropriate to consider the overall ratio (Si + Al):O. In both cases this ratio is 1:2 and therefore, a 3D framework structure is expected. Framework structures also occur in orthoclase, $KAlSi_3O_8$, kalsilite, $KAlSiO_4$, eucryptite, $LiAlSiO_4$ and spodumene, $LiAlSi_2O_6$.

Substitution of Al for Si occurs in many sheet structures such as micas and the clay minerals. The mineral talc has the formula $Mg_3(OH)_2Si_4O_{10}$ and, as expected for an Si:O ratio of 1:2.5, the structure contains infinite silicate sheets. In the mica phlogopite, one quarter of the Si atoms in talc are effectively replaced by Al and extra K^+ ions are added to preserve electroneutrality. Hence, phlogopite has the formula $KMg_3(OH)_2(Si_3Al)O_{10}$. In talc and phlogopite, Mg^{2+} ions occupy octahedral sites between silicate sheets; K^+ ions occupy 12-coordinate sites.

Further complications arise in other aluminosilicates in which Al^{3+} ions may occupy octahedral sites as well as tetrahedral ones. In such cases, one has to have information on the coordination number of aluminium since this cannot be deduced from the formula. One example is the mica muscovite, $KAl_2(OH)_2(Si_3Al)O_{10}$. This is structurally similar to phlogopite, with infinite sheets of constitution $(Si_3Al)O_{10}$ and a (Si + Al):O ratio of 1:2.5. However, the other two Al^{3+} ions replace the three Mg^{2+} ions of phlogopite and occupy octahedral sites. By convention, only ions that replace Si in tetrahedral sites are included as part of the complex anion. Hence octahedral Al^{3+} ions are formally regarded as cations in much the same way as alkali and alkaline earth cations, Table 7.15.

Questions

7.1 Sodium oxide, Na_2O, has the antifluorite structure (Table 7.7). Calculate (a) the sodium–oxygen bond length, (b) the oxygen–oxygen bond length, (c) the density of Na_2O.

7.2 Starting with a cubic close packed array of anions, what structure types are generated by (a) filling all the tetrahedral sites with cations, (b) filling one half of the tetrahedral sites, e.g. the T_+ sites, with cations, (c) filling all the octahedral sites with cations, (d) filling alternate layers of octahedral sites with cations.

7.3 Repeat the above question but with a hexagonal close packed array of anions. Comment on the absence of any known structure in category (a).

7.4 $SrTiO_3$ has the perovskite structure, $a = 3.905$ Å. Calculate (a) the Sr—O bond length, (b) the Ti—O bond length, (c) the density of $SrTiO_3$. What is the lattice type?

7.5 Metallic gold and platinum both have face centred cubic unit cells with dimensions 4.08 and 3.91 Å, respectively. Calculate the metallic radii of the gold and platinum atoms.

7.6 Identify the following cubic structure types from the information on unit cells and atomic coordinates:

(i) MX: M $\frac{1}{2}00, 0\frac{1}{2}0, 00\frac{1}{2}, \frac{111}{222}$
X $000, \frac{11}{22}0, \frac{1}{2}0\frac{1}{2}, 0\frac{11}{22}$

(ii) MX: M $000, \frac{11}{22}0, \frac{1}{2}0\frac{1}{2}, 0\frac{11}{22}$
X $\frac{111}{444}, \frac{313}{444}, \frac{331}{444}, \frac{133}{444}$

(iii) MX: M 000
X $\frac{111}{222}$

(iv) MX_2: M $000, \frac{11}{22}0, \frac{1}{2}0\frac{1}{2}, 0\frac{11}{22}$
X $\frac{111}{444}, \frac{311}{444}, \frac{131}{444}, \frac{113}{444}, \frac{331}{444}, \frac{313}{444}, \frac{133}{444}, \frac{333}{444}$

7.7 Starting from the rock salt structure, what structure types are generated by the following operations:
(i) removal of all atoms or ions of one type;
(ii) removal of half the atoms or ions of one type in such a way that alternate layers only are present;
(iii) replacement of all the cations in the octahedral sites by an equal number of cations in one set of tetrahedral sites.

7.8 Explain why the NiAs structure is commonly found with metallic compounds but not with ionic ones.

7.9 Compare the packing density of the NaCl and CsCl structures for which, in both cases, anion–anion and anion–cation direct contacts occur.

7.10 What kind of complex anion do you expect in the following: (a) Ca_2SiO_4; (b) $NaAlSiO_4$(Al tetrahedral); (c) $BaTiSi_3O_9$; (d) $Ca_2MgSi_2O_7$ melilite; (e) $CaMgSi_2O_6$ diopside; (f) $Ca_2Mg_5Si_8O_{22}(OH, F)_2$ amphibole, tremolite (the OH, F ions are not bonded to Si); (g) $CaAl_2(OH)_2(Si_2Al_2)O_{10}$ mica, margarite (two Al tetrahedral, two Al octahedral); (h) $Al_2(OH)_4Si_2O_5$ kaolinite (Al octahedral, OH not bonded to Si).

References

D. M. Adams (1974). *Inorganic Solids, An Introduction to Concepts in Solid-State Structural Chemistry*, Wiley.

L. Bragg, G. F. Claringbull and W. H. Taylor (1965). *Crystal Structure of Minerals*, Cornell University Press, Ithaca, N.Y.

G. O. Brunner (1971). An unconventional view of the 'closest sphere packings', *Acta Cryst.*, A27, 388.

G. M. Clark (1972). *The Structures of Non-Molecular Solids. A Coordinated Polyhedron Approach*, Applied Science Publishers.
R. C. Evans (1964). *An Introduction to Crystal Chemistry*, 2nd ed., Cambridge University Press.
S. M. Ho and B. E. Douglas (1969). *J. Chem. Ed.*, **46**, 207.
H. Krebs (1968). *Inorganic Crystal Chemistry*, McGraw-Hill.
I. Naray-Szabo (1969). *Inorganic Crystal Chemistry*, Akademiai Szabo.
E. Parthé (1964). *Crystal Chemistry of Tetrahedral Structures*, Gordon and Breach.
Structure Reports, International Union of Crystallography.
Ajit R. Verma and P. Krishna (1966). *Polymorphism and Polytypism in Crystals*, Wiley, New York.
R. Ward (1959). Mixed metal oxides, *Prog. Inorg. Chem.*, **1**, 465.
A. F. Wells (1984). 5th Ed. *Structural Inorganic Chemistry*, Oxford.
A. R. West (1975). *Z. Krist*, **141**, 422–436.
A. R. West and P. G. Bruce (1982). *Acta Cryst.*, **B38**, 1891–1896.
R. W. G. Wyckoff (1971). *Crystal Structures*, Vols 1 to 6, Wiley.

Chapter 8

Some Factors which Influence Crystal Structures